DESIGN AND SYNTHESIS OF BERBERINE DERIVATIVES AS PCSK9 INHIBITOR FOR LIPID REDUCTION

MUNCHALIKA JAITRONG

Graduate School Srinakharinwirot University

2020

การออกแบบและสังเคราะห์อนุพันธ์เบอร์เบอรีนให้เป็นตัวยับยั้ง PCSK9 เพื่อลดระดับไขมัน

มัญชลิกา ใจตรง

ปริญญานิพนธ์นี้เป็นส่วนหนึ่งของการศึกษาตามหลักสูตร
วิทยาศาสตรมหาบัณฑิต สาขาวิชาเคมี
คณะวิทยาศาสตร์ มหาวิทยาลัยศรีนครินทรวิโรฒ
ปีการศึกษา 2563

DESIGN AND SYNTHESIS OF BERBERINE DERIVATIVES AS PCSK9 INHIBITOR FOR LIPID REDUCTION

MUNCHALIKA JAITRONG

A Thesis Submitted in Partial Fulfillment of the Requirements

for the Degree of MASTER OF SCIENCE

(Chemistry)

Faculty of Science, Srinakharinwirot University

2020

THE THESIS TITLED

DESIGN AND SYNTHESIS OF BERBERINE DERIVATIVES AS PCSK9 INHIBITOR FOR LIPID REDUCTION

BY

MUNCHALIKA JAITRONG

HAS BEEN APPROVED BY THE GRADUATE SCHOOL IN PARTIAL FULFILLMENT OF THE REQUIREMENTS FOR THE MASTER OF SCIENCE IN CHEMISTRY AT SRINAKHARINWIROT UNIVERSITY

(Assoc. Prof. Dr. Chatchai Ekpanyaskul, MD.)

Dean of Graduate School

ORAL DEFENSE COMMITTEE

..... Major-advisor

(Assoc. Prof. Dr.Siritron Samosorn)

..... Chair

(Assoc. Prof. Dr.Boon-ek Yingyongnarongkul)

..... Co-advisor

(Dr.Pornthip Boonsri)

..... Committee

(Asst. Prof. Dr.Nuttapon Apiratikul)

Title	DESIGN AND SYNTHESIS OF BERBERINE DERIVATIVES AS PCSK9 INHIBITOR FOR LIPID REDUCTION
Author	MUNCHALIKA JAITRONG
Degree	MASTER OF SCIENCE
Academic Year	2020
Thesis Advisor	Associate Professor Dr. Siritron Samosorn
Co Advisor	Dr. Pornthip Boonsri

Nowadays, Proprotein Convertase Subtilisin/Kexin Type 9 (PCSK9) has become a new target for hypercholesterolemia treatment. PCSK9 is a crucial protein in Low-Density Lipoprotein cholesterol (LDL-C) metabolism by regulating the degradation of hepatic low-density lipoprotein receptors (LDLRs). Recently, two monoclonal antibodies (mAbs) PCSK9 inhibitors were approved by the Food and Drug Administration (FDA). However, no orally administrable small molecule has been approved. In addition, berberine (BBR), an isoquinoline alkaloid, has been reported to reduce total cholesterol levels and decrease PCSK9 expression with no severe side effects. Therefore, a novel series of BBR derivatives was designed based on molecular docking to serve as PCSK9 inhibitors in this work. The binding energy of BBR derivatives was investigated to confirm that all of the designed compounds showed better binding energy and stronger interaction than that of the parent BBR. An *in silico* study was also confirmed that most of the compounds fulfilled drug-likeness properties. Then, eight desired BBR derivatives were successfully synthesized starting from BBR via manich, demethylation, and alkylation reactions. Additionally, BBR derivatives were evaluated for the PCSK9 inhibition activity and the results showed that all of the compounds could down-regulate the PCSK9 expression. Especially, compounds 21 and 24 displayed a high inhibitory effect on PCSK9 by 20-fold higher activity than BBR. Furthermore, the naphthalene substitution at the C-13 position and alkoxy benzenesulfonamide substitution at the C-9 position of BBR significantly affected the inhibition of target enzyme activity. In summary, novel BBR derivatives could be proposed as potential PCSK9 inhibitors for hypercholesterolemia treatment.

Keyword : Berberine, Hypercholesterolemia, Low-density lipoprotein cholesterol, Low-density lipoprotein receptor, Molecular docking, Proprotein Convertase Subtilisin/Kexin type 9

ACKNOWLEDGEMENTS

First and foremost, I would like to express my deepest gratitude to my advisor, Assoc. Prof. Dr. Siritorn Samosorn and my co-advisor, Dr. Pornthip Boonsri, for their invaluable advice. I am incredibly grateful that you continued to have faith in me over the years.

I would also like to thank Prof. Ramida Wattanapoleasin and Ms. Watharaporn Poorahong for their biological technical support.

Besides my advisors, thank you to my committee members: Assoc. Prof. Dr. Boon-ek Yingyoungnarongkul, and Assist. Prof. Dr. Nattapon Apiratikul. Your encouraging words and thoughtful, detailed feedback have been very important to me.

The following financial support: The Center of Excellence for Innovation in Chemistry (PERCH-CIC) and Srinakharinwirot University for providing me scholarships, and Pol. Lt. Col. Phain Charoensuk for partial Tuition Fee support.

I would never forget Dr.Utt Eiamprasert and Assist. Prof. Dr. Sommai Pivsa-Art, Rajamangala University of Technology Thanyaburi for their assistance in providing me the NMR data. I am indebted to the Department of Chemistry, Faculty of Science, Ramkhamhaeng University, for recording the Mass spectra.

Many special thanks also go to my lecturers, colleagues and staff of the Department of Chemistry, Faculty of Science, Srinakharinwirot University for their friendships, encouragement and kind support.

I also wish to express my sincere thanks to Srinakharinwirot University for the laboratory facilities.

Thank you to my friends for cracking jokes even during difficult times and going through anything together. Thank you for always stepping in to help when I need you most.

To my wonderful family who has greatly loved, constantly supported, and being next to me no matter what circumstances. Always thank you.

MUNCHALIKA JAITRONG

TABLE OF CONTENTS

Page

LIST OF TABLES

Page

LIST OF FIGURES

Page

CHAPTER 1
INTRODUCTION

Background

Cardiovascular disease is a high priority in the health care system, especially is the underlying cause of death worldwide. Cardiovascular diseases claim more lives than cancers and chronic respiratory disease combined each year, accounting for approximately 17.8 million deaths in the United States in 2017 (Virani et al., 2020). In addition, ischemic stroke was the highest mortality rate attributable in Europe, North Africa, and Central Asia (American Heart Association, 2021). The risk factor for cardiovascular disease was related to hypercholesterolemia, which refers to high cholesterol levels. Statins are widely commercial cholesterol-lowering drugs. Even though statin therapy is essential for clinical benefits, however, it can cause side effects on the liver, kidney, muscle, and nervous system (ALLEN R. LAST, 2017). For this reason, developing the right candidate for controlling low-density lipoprotein cholesterol (LDL-C) is being continued. Lately, proprotein convertase subtilisin/Kexin type 9 (PCSK9) was discovered and validated as a new potential target for dyslipidemia treatment (Seidah et al., 2014).

PCSK9 plays a crucial role in LDL-C metabolism by controlling the degradation of low-density lipoprotein receptors (LDLRs) in the hepatic cell. Typically, LDL-C is removed from the bloodstream by LDLR. When PCSK9 is activated, it binds to LDLR on the hepatic cell surface and is taken into cells, then released to the lysosome for degradation, which is the same as LDL-C. Because LDLR is decreased, LDL-C level in plasma is increased (Melendez et al., 2017). Therefore, the inhibition of PCSK9 allows elevating the level of LDLR in the liver, resulting in more effective destruction of LDL-C from blood circulation. The US Food and Drug Administration (FDA) has recently approved two novel human monoclonal antibodies (mAbs) as PCSK9 inhibitors for LDL-C reduction: Evolocumab and Alirocumab. They disrupted PCSK9•LDLR interaction efficaciously, with no severe side effects and well-tolerated profiles. However, these drugs are high cost and administrated subcutaneously, limiting factors in patient satisfaction

(Taechalertpaisarn et al., 2018). The great challenge for disruption of PCSK9•LDLR is small-molecule inhibitors, based on the effectiveness of cost and ease of administration (Xu et al., 2019).

The new therapeutic agent development played much attention to a natural products due to their pharmacological activities and less toxicity (Gaba et al., 2021). Berberine (BBR, **1**, Figure 1) is a Chinese herb derived from the protoberberine class of isoquinoline alkaloids. BBR is quite popular in the online market as supplementary food. In recent years, increasing evidence has been reported as BBR can reduce LDL-C in animals, and several clinical studies have also tested in hypercholesterolemic patients with almost none of the side effects (W. Kong et al., 2004; W. J. Kong et al., 2008). In addition, BBR decreased PCSK9 mRNA and protein levels. It was not due to the increase of PCSK9 mRNA degradation, but most likely due to PCSK9 transcription reduction (Cameron et al., 2008; Dong et al., 2015). Therefore, BBR might be a potential lead compound for a lipid-lowering agent and required structure modification to improve the activity. BBR derivatives were designed and synthesized in this study, and their PCSK9 inhibitory activity were evaluated.

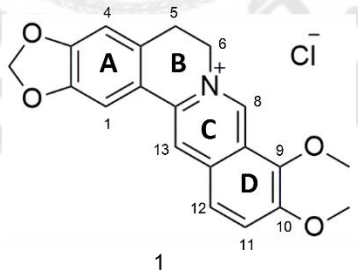

1

Figure 1 Structure of Berberine (BBR)

Molecular docking plays a crucial component in the drug discovery toolbox. In molecular modelling, docking is a method that predicts the affinity and activity of a given small molecule drug candidate when bound in an active site or binding pocket of the macromolecular target such as protein. Then, this protein matches along to be a perfect fit to form a stable complex. The scoring feature or force field based on the free binding

energy is applied to select the best fit or the best drug from an array of options. The protein is kept rigid and fixed during docking, whereas the ligand is allowed flexibility in this module. The behaviour of ligand in the binding pockets of target proteins can be described as its biological function. In this study, molecular docking was aided in designing BBR derivatives based on structure-activity relationships and predicting their biological activity. Accordingly, the desired molecules were synthesized, and their PCSK9 inhibitory activity were evaluated.

Objectives of the Study

1. To design BBR derivatives using PCSK9 based computer-aided drug design.
2. To study the interaction between BBR derivatives and proteins, PCSK9, using molecular docking.
3. To synthesize the selected BBR derivatives.
4. To evaluate the PCSK9 inhibitory activity of the synthesized BBR derivatives.

Significance of the Study

'Health is wealth' that is the fact from the past until today. One of the most critical issues is health problems, predominantly obesity and overweight because it was the cause of cardiovascular disease induced by hypercholesterolemia. PCSK9 is a new potential target for dyslipidemia treatment. However, a studied and clinically approved approach of the small molecules PCSK9 inhibitor is not yet sufficient. Also, several natural products as BBR have been suggested to improve lipid metabolism. Therefore, BBR was implied to be a potential therapeutic agent. In this study, BBR derivatives were designed and successfully synthesized. Finally, all of the desired compounds were evaluated for their activity as a novel PCSK9 inhibitor that can further develop small-molecule PCSK9 inhibitors in the future.

Scope of the Study

1. BBR derivatives were designed using PCSK9 based on computer-aided drug design by improving the lipophilicity with naphthalene moiety at the C-13 position and an alkoxy benzenesulfonyl group at C-9. In addition, the effect of substituents on the benzenesulfonyl ring was studied.

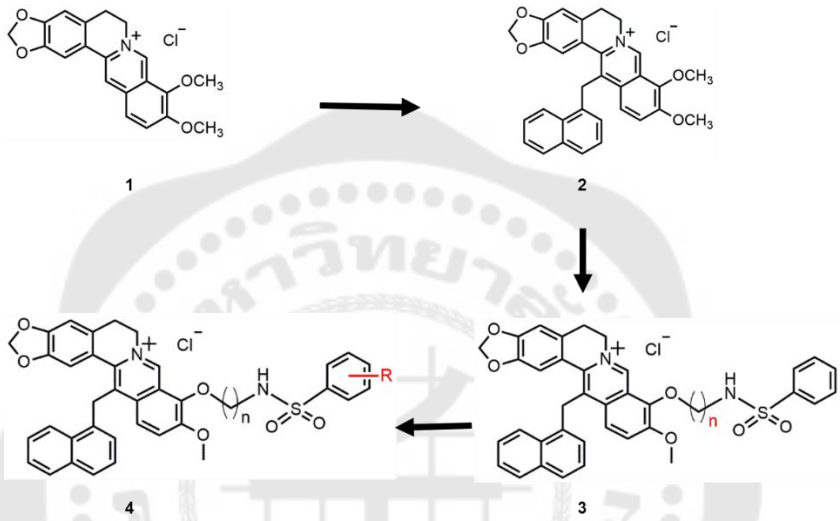

Figure 2 Computer-aided drug design of BBR derivatives.

2. The binding pose and interactions between BBR derivatives and PCSK9 were evaluated.

3. The selected BBR derivatives were synthesized and evaluated bioactivities as PCSK9 inhibitors.

CHAPTER 2
LITERATURE REVIEW

Proprotein convertase subtilisin/Kexin 9 (PCSK9)

Overweight and obesity are some of the fundamental health problems leading to morbidity and mortality. According to the World Health Organization (WHO), the leading cause of death worldwide is cardiovascular disease (CVD). Atherosclerosis and Stroke are essential conditions of CVD, develop when the blood supply to a part of the heart or brain is cut off due to the blood vessels is being narrows, and clots, making it harder for blood to flow through. Cholesterol is one of the causes of the narrowing of a blood vessel. Cholesterol is the most abundant steroid family in the body that is a lipid with a unique structure. It is an amphiphilic tetracyclic hydrocarbon that consists of a hydrophobic hydrocarbon head and a hydrophilic hydroxyl tail. Cholesterol is derived from diet and synthesized in the body, primarily in the liver of mammals. Cholesterol is transported to other parts of the body through bloodstream. However, it is insoluble in blood and must be packaged on proteins called Lipoproteins. When cholesterol is within these lipoproteins, it is referred to as Low-density lipoproteins (LDL).

LDL is an essential lipoprotein that consists of cholesterol esters, triglycerides, phospholipids, and apolipoproteins B-100 (Apo-B100). Most of the cholesterol in the circulating blood system, which the liver and most other tissues used to make many functions, such as a critical part of the cell membrane, bile acid source, and steroid hormones, were carried by LDL. In addition, LDL was delivered into cells through the Low-density lipoprotein receptors (LDLRs) expressed on the hepatic cell surface via endocytosis. After internalization, LDL is degraded in lysosomes and released to travel in the bloodstream as free cholesterol. Nonetheless, cells have limited LDL requirements. As a result, it is sometimes harmful when high cholesterols are also called hypercholesterolemia—excess cholesterol build-up a plaque on the wall that narrows the blood vessel (Jeon & Blacklow, 2005). Two ways of hypercholesterolemia treatment: one is lifestyle changes, a Heart-healthy diet, get moving, lose weight and stop smoking. Another way is to take cholesterol-lowering drugs to effect in controlling cholesterol.

Several drugs have been widely used for reducing LDL-C levels (Soran et al., 2017). Statin therapy or 3-hydroxy-3-methylglutaryl -coenzyme A (CoA) reductase (HMGCR) inhibitor is one of the cornerstones that have been widely regarded as the first line for LDL-C reduction (Krahenbuhl et al., 2016). Even though statin therapy is essential for clinical benefits in the long term, it is well tolerated in most individuals. However, there is a side effect: gastrointestinal intolerance, upper respiratory symptoms or headaches, liver abnormalities, and muscle aching limiting their use.

In addition, statin treatment is insufficient to some patients with very high baseline LDL-C levels. Consequently, they fail to attain desirable LDL-C target values. (Xu et al., 2019). Familial hypercholesterolemia (FH) constituted one of the inherited metabolic diseases in the difficult-to-treat patient groups. FH is dyslipidemia characterized as an autosomal monogenic disorder caused by mutations in genes that code to remove LDL proteins responsible for circulation. Account for most causes of FH is the mutations in LDLR (encoding the LDL receptor) and APO B (encoding apolipoprotein B100 (apoB100)) (Melendez et al., 2017).

Proprotein convertase subtilisin/Kexin-9 (PCSK9) was the third gene to be discovered as the cause of FH in 2003. PCSK9 is on chromosome 1p32.3, the ninth member of the proprotein convertase family (Seidah et al., 2014). PCSK9 encodes an inactive glycoprotein (pre-PCSK9) with 692 amino acids and is synthesized as a 74 kDa. Four components of PCSK9 comprised with a signal peptide (SP; amino acids 1-30), N-terminal prodomain (31-152), a subtilisin-like catalytic domain (amino acids 153-404), and C-terminal CHR domain (CHRD; amino acids 405-692) (Melendez et al., 2017) as shown in Figure 3.

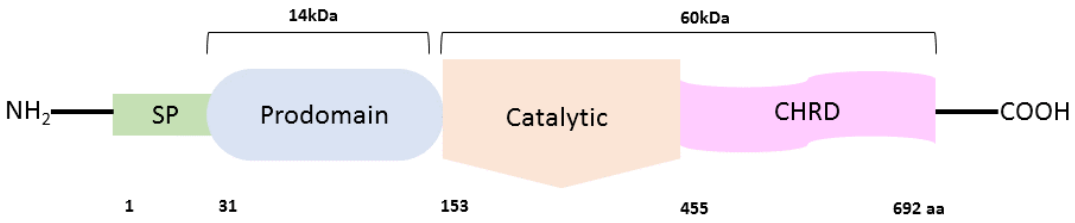

Figure 3 Proprotein convertase subtilisin/Kexin 9 (PCSK9) protein domains.

Source: Melendez, Q. M., Krishnaji, S. T., Wooten, C. J., & Lopez, D. (2017). Hypercholesterolemia: The role of PCSK9. Arch Biochem Biophys, 625-626, 39-53.

Firstly, pre-PCSK9 is cleaved the signal peptide (1-30) domain in the endoplasmic reticulum (ER). Subsequently, amino acids 31-692 are formed to pro-PCSK9. Then, autocatalytic cleavage between Gln152 and Ser153 released the prodomain (14 kDa) from the N-terminal region. However, the propeptide and the catalytic domain remain tightly and must obstruct other proteins to the active site of PCSK9. Therefore, the autocatalytic cleavage activates it to mature secretory PCSK9 in the Golgi apparatus and allows the non-covalently bound PCSK9/prodomain complex departure from ER (Xu et al., 2019). Finally, PCSK9 migrates via the secretory pathway until it is secreted into the bloodstream, as shown in Figure 4. Typically, PCSK9 expression occurs when hypocholesterolemia and human plasma PCSK9 levels have been reported varying from 30 ng/mL up to 4 mg/mL (Melendez et al., 2017).

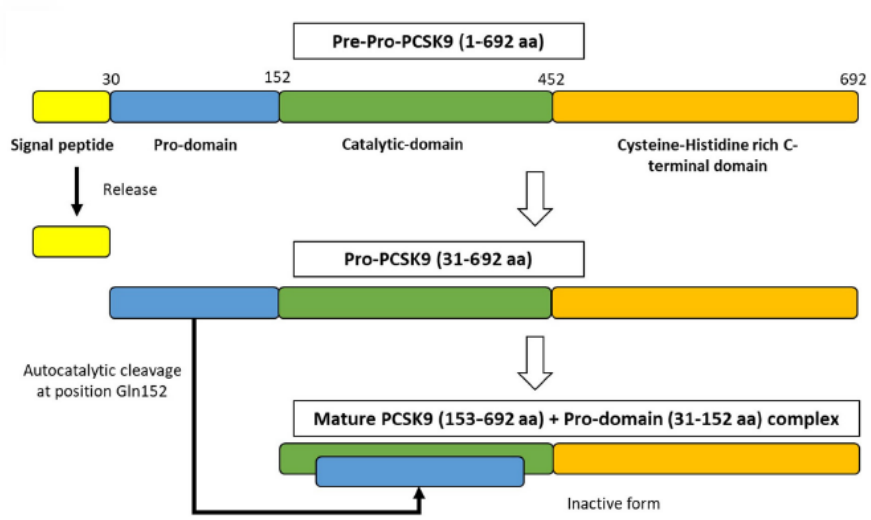

Figure 4 The synthesize of PCSK9 protein in the endoplasmic reticulum

Source: Nishikido, T., & Ray, K. K. (2018). Non-antibody Approaches to Proprotein Convertase Subtilisin Kexin 9 Inhibition: siRNA, Antisense Oligonucleotides, Adnectins, Vaccination, and New Attempts at Small-Molecule Inhibitors Based on New Discoveries. Front Cardiovasc Med, 5, 199.

Very high plasma concentrations of LDL characterize the gain of function mutation (GOF) in the PCSK9 that promotes the LDLR degradation by forming a complex with them. In terms of mechanism (Figure 5), on the hepatic cell surface without PCSK9, LDLR bind with LDL-C. The complex is then transported to the endosomes via endocytosis and releases the LDL to the lysosome to degrade cholesterol and amino acids. In contrast, LDLRs are transported to the cell surface and do it all over again. With PCSK9, the catalytic domain of PCSK9 is bound with the epidermal growth factor A (EGF-A) domain of the LDL receptors on the cell membrane under the neutral condition and took into cells like LDL receptor cycle. Interestingly, a pH inside the endosome changes into acidic preferred for the PCSK9-LDLR complex to binding tightly increases 150-170 folds compared to the cell membrane. Thus, LDLR degradation occurred in lysosomes without being recycled to the hepatic cell surface (Ogura, 2018).

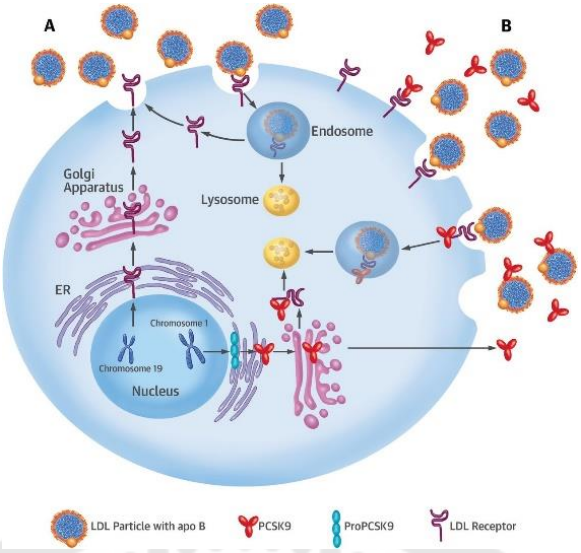

Figure 5 PCSK9·LDLR interaction

Source: Rosenson, R. S., Hegele, R. A., Fazio, S., & Cannon, C. P. (2018). The Evolving Future of PCSK9 Inhibitors. J Am Coll Cardiol, 72(3), 314-329.

Interestingly, the relation between PCSK9 and statin treatment was demonstrated via the steroid response element-binding protein-2 (SREBP-2) pathway. SREBP-2 is a transcription factor involved with cholesterol homeostases. Statin increased the clearance of LDL from the bloodstream by HMGCR inhibition. Then, SREBP-2 was activated and bound to a sterol response element (SRE) in the PCSK9 gene promoter region when intracellular cholesterol was decreased for upregulating the PCSK9 transcription, as shown in Figure 6 (Jeenduang, 2014).

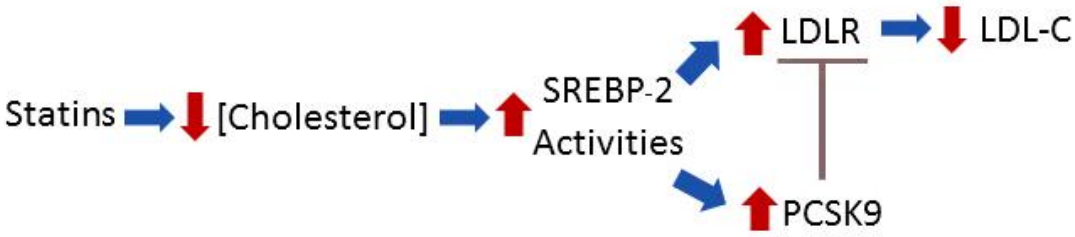

Figure 6 Regulation of LDLR and PCSK9 expression in the hepatic cell by statin.

Source: Olivia May. (2008). Mediating Cholesterol Homeostasis through SREBP2 LDLR PCSK9 Signalling from Cayman Chemical

PCSK9 Inhibitor

At present, PCSK9 inhibitor is a new agent for controlling LDL-C in the same way to inhibit LDLR degradation. Alirocumab and Evolocumab are the first two human anti-PCSK9 monoclonal antibodies (mAbs) approved by the US Food and Drug Administration (FDA)(Melendez et al., 2017). The previous study reported that patients the primary hyperlipidemia and clinical atherosclerotic CVD initially received 4-week statin therapy. Then, patients were randomized to subcutaneous injections of evolocumab 140 mg/2 weeks, evolocumab 420 mg/month or placebo for 12 weeks. After 4 weeks, the mean baseline LDL-C level was 108 mg/dL. The result showed that evolocumab 140 mg/2 weeks reduced a 71% in mean LDL-C, and evolocumab 420 mg/month decreased LDL-C a 63% compared to placebo. Thus, anti-PCSK9 mAbs can be potentially used as an add-on to statins treatment in human clinical trials, which are efficacious and have no noticeable side effects (Fala, 2016). Even though injectable antibody therapeutics resisted the PCSK9•LDLR protein-protein interaction (PPI) was a success. However, the interest in PCSK9 inhibitor development based on the mode of administration, cost, shelf life, and immunogenic response issues is still grown. The highly desirable preferred modality alternative therapeutic agent would be an orally available small-molecule inhibitor (Taechalertpaisarn et al., 2018).

In 2016, the peptic and tryptic peptides from lupin protein were treated with HepG2 cells to observe the precursor PCSK9 protein reduction and decrease the

PCSK9 protein secretion. The mild hypercholesterolaemic subjects consumed lupin protein (30 g/day) for 4 weeks. The results showed that the final circulating PCSK9 level was equal to 8.5% compared to the average PCSK9 plasma levels baseline at 82.9 ± 22.2 ng/mL, whereas total cholesterol (TC) reduction was 4.2%. Furthermore, peptic and tryptic lupin peptides significantly decreased the hepatic nuclear factor 1-alpha (HNF1-α) (Carmen Lammi et al., 2016).

Black raspberry extract (BRE) was investigated to inhibit PCSK9 transcription. The results reported that BRE modulates induced LDL-C uptake and LDLR expression. Furthermore, BRE also repressed PCSK9 expression. In addition, BRE co-treatment with simvastatin inhibited PCSK9 secretion better than simvastatin alone. Therefore, simvastatin and BRE are synergic for the anti-hypercholesterolemia treatment. Moreover, BRE involved with PCSK9 transcription caused no significant change in the SREBP-2 pathway but suppressed expression and transcriptional of the HNF1α transcription factor (Song et al., 2018).

Isolated compounds of *Nauclea latifolia* include three alkaloids, and two terpenoids were evaluated for their LDL uptake effect in HepG2 cells. The results showed that *3R*-3,14-dihydroangustoline (**5**) showed relatively good promoting LDL uptake activity, whereas its *S*-isomer less displayed that activity. Furthermore, compound **5** also promoted the LDLR expression while induced the PCSK9 down-regulation in a dose-dependent manner (Aggrey et al., 2019).

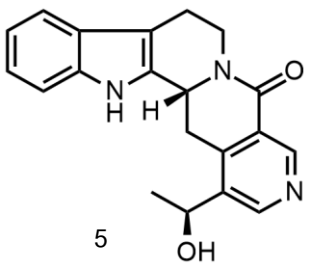

5

Figure 7 Structure of compound **5**

In 2019, C. Wu et al. designed and synthesized a novel series of indole-containing tetrahydroprotoberberine derivatives (THPBrs). All indole-containing THPBrs have investigated the ability to increase PCSK9 down-regulating via structure-activity relationship (SARs) exploration, which led to identifying a highly potent PCSK9 modulator. Compound **6** (IC_{50} = 1.34 μmol/L) exhibited excellent activities, promoting a 2.37-fold (5 μmol/L) LDL uptake and promoting LDLR expression in the hepatic cell in a dose-dependent manner optimal 2.06-fold at 5 μmol/L. *In vivo* study, after 21 days of treatment, high-fat diet (HFD)-induced hyperlipidemic hamster by oral gavage, compound **6** displayed excellent hypolipidemic potency that reduced 36.7% of TC and reduced 41.4% in serum LDL-C and showed a unique pharmacokinetic profile which an oral bioavailability of 21.9% (Wu et al., 2019).

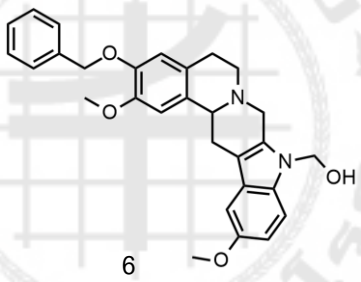

6

Figure 8 Structure of compound **6**

T9D8A_1, a new analogue of Lupin peptide (T9), was substituted by amino acids to increase the structural complementarity between T9 and $PCSK9^{D374Y}$. *In silico*, T9D8A_1 showed the highest binding affinity. In addition, the obtained results showed that T9D8A_1 increased LDLR expression by 84% and re-established the LDL uptake level more than T9 35-fold on the hepatic cell surface (Lammi et al., 2019).

CVI-LM001 (**7**), the fluorobenzenesulfonate derivative of corydaline, was studied in a preclinical trial. The results indicated that compound **7** showed the hypolipidemic effect in hypercholesterolemic animal models. In addition, the mechanism studies showed that compound **7** increased LDLR expression and PCSK9 down-regulation (Xu et al., 2019).

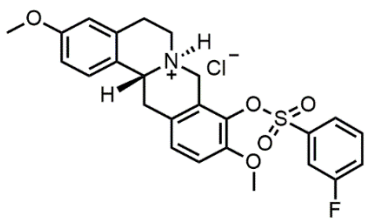

7

Figure 9 Structure of compound **7**

Compound **8** was an indole analogue that was substituted with a sulfonamide alkyl linked with morpholine. Interestingly, compound **8** showed PCSK9 inhibition activity with EC_{50} values less than 1 nM (Xie et al., 2020).

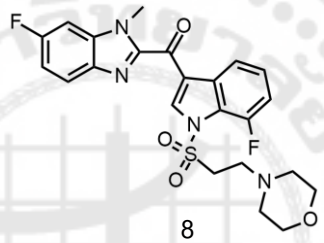

8

Figure 10 Structure of compound **8**

Berberine

Berberine (BBR) has commonly been used in Chinese medicine as a traditional medicinal herb without toxicity due to exerting several pharmacological and therapeutic effects, including antimicrobial, antitumor, immunomodulatory properties, anticancer, antihyperglycemic, antiheart failure functions, and especially its anti-hypercholesterolemia effect. BBR is an isoquinoline alkaloid (2, 3-methylenedioxy-9,10-dimethoxyprotoberberine chloride) that belongs to protoberberines in several plants like *Berberis vulgaris*, *Coptis chinensis*, *Berberis aristata*. Interestingly, BBR has been reported to reduce serum LDL, which was mediated by up-regulated at the post-transcriptional LDLR expression mechanism distinct from cholesterol-lowering statin drugs, through stabilising the LDLR mRNA in an extracellular matrix signal-regulated kinase-dependent manner (W. Kong et al., 2004). In a clinical trial, BBR decreased LDL-C and TC levels and also improved dyslipidemia in HFD rats. In addition, BBR significantly

increased High-density Lipoprotein cholesterol (HDL-C) levels. Moreover, it reduced the secretion and expression of PCSK9 (Pirillo & Catapano, 2015). BBR could have dual actions by prolonging its mRNA half-life; in another way, increasing the abundance of protein through the blockage of PCSK9-mediated degradation in LDLR metabolism (H. Li et al., 2009). Another approach to knock down PCSK9 expression is to exploit endogenous gene regulation systems through reducing transcription factors of the PCSK9 gene (Duff & Hooper, 2011), including members of the SREBP family and hepatocyte nuclear factor 1α (HNF1α; that recognizes the site explicitly between Sp1 and SRE on the PCSK9 pro¬moter) which work cooperatively with SREBP-2 in PCSK9 transactivation. Hence, PCSK9 transcription was repressed due to the interac¬tion of two transcription factors with their binding sequence of PCSK9 promoter reduction (Nishikido & Ray, 2018). Recently, *in vivo* studies using hyperlipidemic mice demonstrated that HNF-1α and SREBP-2 levels simultaneously reduced by BBR via the ubiquitin-proteasome system (UPS) and the autophagy-lysosomal pathway blocking to reduce the hepatic HNF1α protein levels without affecting the mRNA levels that stabilizes the LDLR mRNA (He et al., 2017).

Biological activities of berberine and berberine derivatives as PCSK9 inhibitors.

Cameron et al. were the first group who reported that BBR suppressed PCSK9 mRNA and protein levels in a time and dose-dependent manner. The two possible PCSK9 inhibition mechanisms of BBR were proposed that induced PCSK9 mRNA downregulation or decreased PCSK9 gene transcription. Furthermore, the obtained results showed that a combination of BBR and mevastatin treatment increased LDLR mRNA and protein levels. Unfortunately, the effect of BBR on PCSK9 mRNA transcription via the SREBP pathway expression was remained to be fully explored (Cameron et al., 2008).

An earlier report showed that BBR increased LDLR expression and down-regulated PCSK9 transcription by inhibiting the binding of HNF1α to the sequence of the

HNF motif located between the SRE and Sp1 binding sites. As a result, the cellular abundance of HNF1α and SREBP-2 were decreased (H. Li et al., 2009).

Jia et al. showed that BBR significantly improved lipid profile and reduced body weight gain after six weeks of treatment. Besides, BBR decreased the serum levels of triglyceride. In the same way, BBR increased mRNA levels of LDLR and SREBP-2. In addition, it induced HDL-C expression, whereas down-regulated HNF1 transcription in the hepatic cell (Jia et al., 2014).

In 2015, Dong et al. studied the inhibition of PCSK9 gene expression. The result showed that BBR accelerated HNF1α protein degradation in cultured cells and animal models by inhibiting the binding of HNF1α to the HNF1 (-), as shown in Figure 11. Moreover, SREBP2 transcription was inhibited from binding with the SRE-1 site of PCSK9 promoter by BBR (-), while it was up-regulated through statin (-). (Dong et al., 2015)

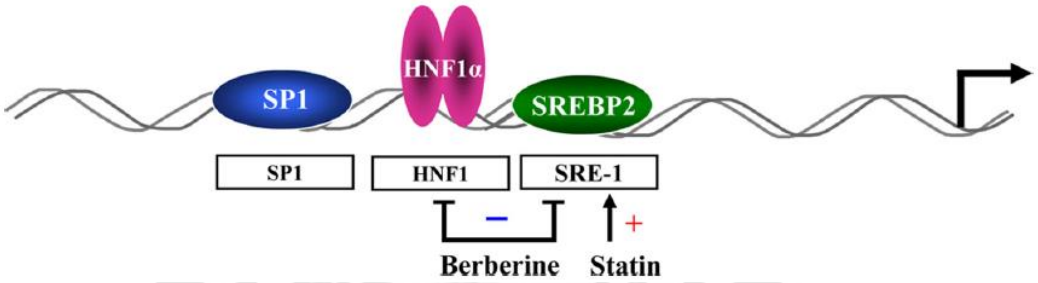

Figure 11 Regulation of human PCSK9 promoter by statin and BBR.

Source: Li, H., Dong, B., Park, S. W., Lee, H. S., Chen, W., & Liu, J. (2009). Hepatocyte nuclear factor 1alpha plays a critical role in PCSK9 gene transcription and regulation by the natural hypocholesterolemic compound berberine. J Biol Chem, 284(42), 28885-28895.

Molecular Docking

(*R*)-*N*-(isoquinolin-1-yl)-3-(4-methoxyphenyl)-*N*-(piperidin-3-yl) propanamide (R-IMPP, **9**) was identified as a new anti-PCSK9 small molecule by High-throughput screening (HTS) through a phenotypic screen from 2.55 million compounds. Compound **9** demonstrated that it could not decrease transcription or degradation of

PCSK9 but increased LDL-C uptake in hepatoma cells by upregulating LDLR levels. (Petersen et al., 2016).

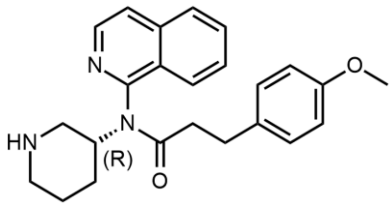

9

Figure 12 Structure of compound **9**

In 2017, S. Sultan Alvi et al. evaluated the Lycopene to PCSK9 inhibitor in HFD rats via the modulation of the gene involved with cholesterol homeostasis and examined the regulation of PCSK-9 expression. In silico, lycopene was docked into the PCSK9 with the EGF(A) portion of LDLR (PDB: 2P4E) compare to atorvastatin. Additionally, lycopene-PCSK9 and Atorvastatin-PCSK9 complexes showed the binding energies of -493.93 and -524.60, respectively. The most important outcome from these observations was identical amino acid residues such as Trp460, Val459, Thr458, Arg457, Ala477, Arg411, Glu331, Pro330, and Arg439 in order to occupy the binding pocket of PCSK9. For the hyperlipidemia induction study of Lyc, rats were divided randomly and equally in 3 groups for intervention study: Lyc-1 (5 mg/kg B.W./rat/day), Lyc-2 (10 mg/kg B.W./rat/day), and Lyc-3 (50 mg/kg B.W./rat/day). The result showed that Lyc-3 group significantly maximum reduced plasma LDL-C levels and increased the HDL-C level from 12.1±0.74 to 25.1±0.39 mg/dL. In addition, it also down-regulated HMGCR and PCSK9 genes expression by 3.40 and 2.26 folds, respectively. Moreover, Lyc3 upregulated 1.85 folds of LDLR expression after 30 days of treatment (Sultan Alvi et al., 2017).

In 2018, LDLL-1dlnr (**10**) was designed by comparing LDLR side chains at the PCSK9•LDLR interface using the Exploring Key Orientations approach. In addition, compound **10** was subjected to an ELISA assay. The results showed that compound **10** increased PCSK9 inhibition by upregulating LDL uptake and LDLR expression with no toxicity up to 100 μmol/L in cell culture. (Taechalertpaisarn et al., 2018).

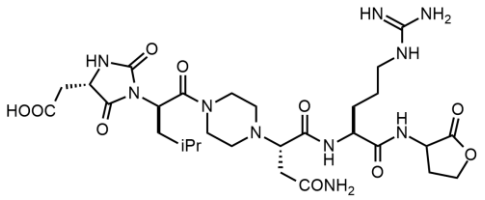

10

Figure 13 Structure of compound **10**

The docking studies used the BREED algorithm to design novel hybridized ligands. Berberine methine tetrahydro-2 vinyl 4 H 3 dithin-berberine methine tetrahydro-rosuvastatin (**11**) showed the best Cdocker energy (-13.552 kcal/mol). Interaction between compound **11** and PCSK9 performed that the carboxylic-CO and pyridine N atom generated two hydrogen bonds with Arg97 residue. Furthermore, the carboxylic-OH and phenol also interacted hydrogen bond through His139, and Arg93, respectively. The CO carbonyl group formed interaction to Thr94 via van der Waals (Puratchikody et al., 2019).

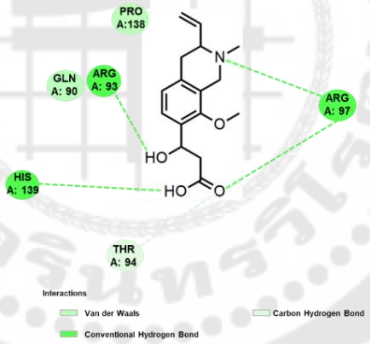

Figure 14 Two-dimension interaction of compound **11** with amino acid residues.

Source: Puratchikody, A., Irfan, N., & Balasubramaniyan, S. (2019). Conceptual design of hybrid PCSK9 lead inhibitors against coronary artery disease. Biocatalysis and Agricultural Biotechnology, 17, 427-440.

CHAPTER 3
RESEARCH METHODOLOGY

General Instrument

Bruker 500 MHz Nuclear magnetic resonance (NMR) spectroscopy (AVANCE NEO)

High-performance Computer (VivoBook S, ASUS)

SkanItTM Software for Microplate Readers Version 5.0 (ThermoScientific)

Sealed tube

UV Spectrophotometer

Chemical

Acetonitrile (AR grade, ACI Labrscan)

2-Bromoethylamine hydrobromide (>98.0%, Tokyo Chemical Industry co., Ltd.)

1-(chloromethyl)naphthamethyl (90%, Sigma Aldrich)

Dimethyl formamide (99.5%, Merck)

Benzenesulfonyl chloride (>99.0%, Tokyo Chemical Industry co., Ltd.)

p -toluenesulfonyl chloride (>99.0%, Tokyo Chemical Industry co., Ltd.)

4-methoxybenzenesulfonyl chloride (99.0%, Sigma Aldrich)

4-fluorobenzenesulfonyl chloride (>97.0%, Tokyo Chemical Industry co., Ltd.)

4-nitrobenzenesulfonyl chloride (>98.0%, Tokyo Chemical Industry co., Ltd.)

4-cyanobenzenesulfonyl chloride (>98.0%, Tokyo Chemical Industry co., Ltd.)

Berberine (chloride salt) ($\geq$90 %, Sigma-Aldrich Chemical Co.)

Silica gel (SiliCycle, SILSAFLASH G60, 230-400 mesh)

Aluminium oxide 90 active neutral (E. Merck, 70-230 mesh)

TLC plates (20X20, 0.5 mm thick, E. Merck)

The LEGEND MAX™ Human PCSK9 ELISA kit, BioLegend, Catalog Number 443107

Method

Molecular docking of PCSK9

Ligand preparation

The 3D structure of the BBR was downloaded from the PubChem Compound Database (National Center for Biotechnology Information; https://pubchem.ncbi.nlm.nih.gov/). The BBR and derivatives structures called ligands were carried out to minimize energy at the B3LYP/6-31G (d,p) using the G09 program (M. J. Frisch, 2009) to stabilize structures. The stable 3D ligands were prepared in combinations with nonpolar hydrogens, gasteiger charges, rotatable bonds based on the ADT program.

Protein preparation

The X-ray crystal structure of the human PCSK9, which was constructed in the presence of the EGF(A) domain of the LDLR at neutral pH (PDB code 3GCX) (Taechalertpaisarn et al., 2018) with a resolution of 2.70, was downloaded from the Protein Data Bank (PDB) [Research Collaboratory for Structure Bioinformatics (RCSB), (http://www.rcsb.org/pdb)]. Firstly, protein structures were checked for missing atoms, residues, bonds, and contacts. Then, some water and co-factors were removed by using the Discovery studio 2020 client (BIOVIA, 2020). Finally, the AutoDock Tools program (ADT) 1.5.6 (M.F. Sanner, 1999) was used to add hydrogen atoms to a target protein to obtain protein.pdbqt format.

Molecular docking

Previously described, BBR and its derivatives (ligand) were designed and optimized to get stabilized structures. BBR derivatives and PCSK9 protein, which were prepared, loaded into the ADT, and replaced the EGF(A) of the LDL receptor that binds to PCSK9 with ligand form ligand.pdbqt format. The docking grids were also prepared using ADT with a grid box created with 60 x 60 x 60 points whose center coordination was 13.805, -36.325, and 0.195 (x, y, z) and a resolution 0.375 Å. After the grid, potential maps were calculated using module AutoDock 4.2 (G. M. Morris, 2009). Then, the ligands were docked to human PCSK9, obtaining the binding interaction of the complex structure. Default docking parameters were applied using a genetic algorithm approach (ga),

except that 150 ga runs were used with 2,500,000 as the maximum number of evaluations and set a root mean square deviation (RMSD) tolerance to 2.0 Å. The docking results were then clustered based on the RMSD between the atoms' coordinates in a given ligand and were ranked based on the calculated binding energy. The results were analyzed to find the lowest binding free energy with the best-clustered compounds. Post-docking analyses were visualized using the Discovery Studio program, which showed the binding pose, the intermolecular protein-ligand interaction, and interaction radii of bonding distances of <5 Å position the docked ligand.

Analysis of drug-likeness

Biological systems in a living organism are furnished with a heterogeneous phase such as water, serum protein, lipid particles that influence the molecule behavior in drug transport processes (Alam et al., 2013). Nowadays, the physicochemical properties of molecules (Bakht et al., 2010) play an essential role as a tool in drug design. There are various guidelines for small molecules analysis as a therapeutic agent from an oral bioavailability perspective, the Lipinski rule most well-known. A compound should be fallen within the rule of five criteria: molecular weight (MW), Log partition coefficient (LogP), number of hydrogen bond acceptors (HBA) and donors (HBD), molecular polar surface area (TPSA), and number of rotatable bonds (nRB). The designed compounds in this study were calculated by using free software (http://www.molinspiration.com/).

Synthesis

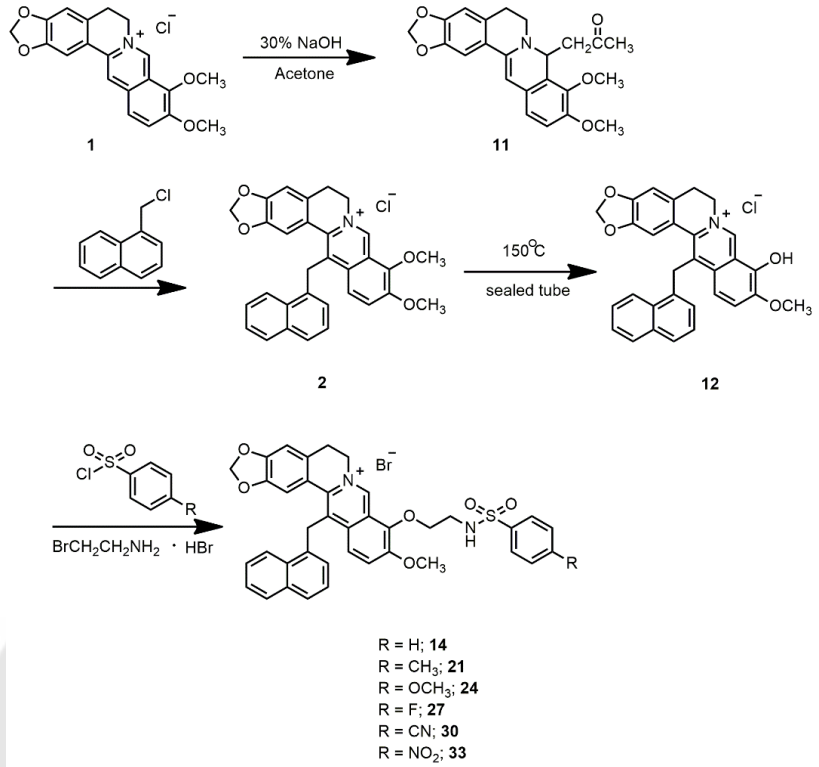

Figure 15 Synthesis pathway of the desired compounds.

Synthesis of 13-(1-naphthalenylmethyl) berberine (2)

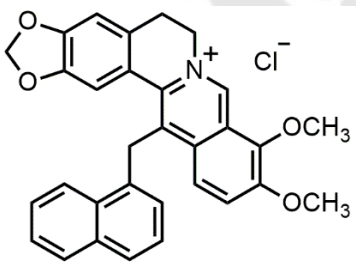

To a suspension of berberine (2.00 g, 5.38 mmol) was suspented in acetone (60 mL), was added 30% aqueous sodium hydroxide (70 mL). The mixture was heated at 65 °C for 2 h. The reaction mixture was concentrated and then poured into ice water (300 mL); the precipitate was filtered and dried to give 8-acetonyldihydroberberine (1.80 g, 0.42 mmol) as a pale yellow solid, which was then dissolved in acetonitrile (20 mL) and add 1- (chloromethyl)naphthamethyl (1 mL, 6.68 mmol). The reaction was refluxed at 80 °C for 6 h. The mixture was then concentrated and chromatographed on silica column (6% MeOH in DCM) to give **2** (1.20 g, 51.3%) as a yellow solid. ^{1}H NMR ($CDCl_3$, 500 MHz): δ 10.62 (s, 1H, 8-H), 7.56 (d, 1H, *J* = 9 Hz, 11-H), 7.43 (d, 1H, *J* = 9 Hz, 12-H), 6.89 (s, 1H, 1-H), 6.82 (s, 1H, 4-H), 6.8-8.1

(m, 7H, naphthyl Ar-H), 5.85 (s, 2H , OCH_2O), 5.26 (brs, 2H, 6-H), 4.97 (s, 2H, CH_2- Ar), 4.37 (s, 3H, 9-OCH_3), 3.95 (s, 3H, 10-OCH_3), 3.28 (brs, 2H, 5-H). HRMS (ESI): m/z calcd for $C_{31}H_{26}NO_4$ $[M]^+$: 476.1856; found: 476.1858.

Synthesis of 13-(1-naphthalenylmethyl) berberrubine (12)

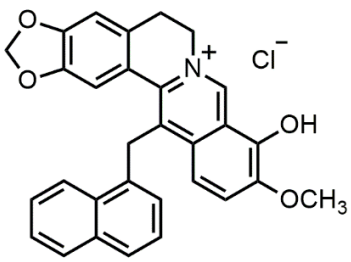

A yellow suspension of 13-(1-naphthalenylmethyl) berberine (1.20 g, 2.34 mmol) in dimethyl formamide (DMF, 3 mL) in a sealed tube was heated at 150 °C for 2 h. The resulting red solution was cooled to room temperature. The mixture was concentrated and chromatographed on neutral alumina column (3 % MeOH in DCM) to give **12** (800 mg, 68.6%) as a red solid. ^{1}H NMR ($CDCl_3$, 500 MHz): δ 9.35 (s, 1H, 8-H), 7.02 (d, 1H, *J* = 8.5 Hz, 11-H), 7.02 (d, 1H, *J* = 8.5 Hz, 12-H), 7.00 - 8.10 (m, 7H, naphthyl Ar-H), 6.87 (s, 1H, 1-H), 6.75 (s, 1H, 4-H), 5.82 (s, 2H, OCH_2O), 4.76 (s, 2H, CH_2- Ar), 4.39 (brs, 2H, 6-H), 3.82 (s, 3H, 10-OCH_3), 3.03 (brs, 2H, 5-H). HRMS (ESI): m/z calcd for $C_{30}H_{24}NO_4$ $[M]^+$: 462.1700; found: 462.1701.

Synthesis of compound 14

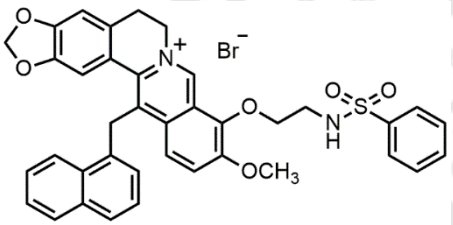

To a suspension of benzenesulfonyl chloride (0.29 mL, 2.28 mmol) in ethyl acetate (3 mL), 2-bromoethylamine hydrobromide (606 mg, 2.96 mmol) and triethylamine (0.64 mL, 4.56 mmol) were added at 0 °C. The mixture was then stirred at room temperature for 4 h, then concentrated under reduced pressure. The crude product was purified by column chromatographed on silica gel (DCM) to give a corresponding intermediate reagent. A mixture of compound **12** (100 mg, 0.2008 mmol) and anhydrous potassium carbonate (K_2CO_3) (28 mg, 0.2008 mmol) was added to anhydrous acetonitrile (10 mL). The resulting red suspension was stirred in an oil bath, followed by adding the intermediate reagent (85.7 mg, 0.32 mmol). The reaction mixture was refluxed at 80 °C for 2 days. The mixture color was changed from red to yellow and monitored by thin-layer chromatography (TLC) analysis.

Subsequently, the mixture product was then concentrated under reduced pressure and chromatographed on silica column (3% MeOH/DCM) to give **14** (50.9 mg, 34.9%) as a yellow solid. ^{1}H NMR ($CDCl_3$, 500 MHz): δ 10.90 (s, 1H, 8-H), 8.68 (t, 1H, *J* = 5.5 Hz, N-H), 7.55 (d, 1H, *J* = 9.4 Hz, 11-H), 7.46 (d, 1H, *J* = 9.3 Hz, 12-H), 7.40 - 8.10 (d, 4H, *J* = 8.12 Hz, benzene Ar-H), 6.93 (s, 1H, 1-H), 6.84 (s, 1H, 4-H), 6.8-8.2 (m, 7H, naphthyl Ar-H), 5.87 (s, 2H , OCH_2O), 5.31 (brs, 2H, 6-H), 5.00 (s, 2H, CH2-Ar), 4.66 (t, 2H, *J* = 4 Hz, 9-OCH_2), 3.94 (s, 3H, 10-OCH_3), 3.43 (s, 2H, OCH_2CH_2NH), 3.27 (brs, 2H, 5-H). HRMS (ESI): m/z calcd for C38H33N2O6S [M]+: 645.2054; found: 645.2022.

Synthesis of compound 21

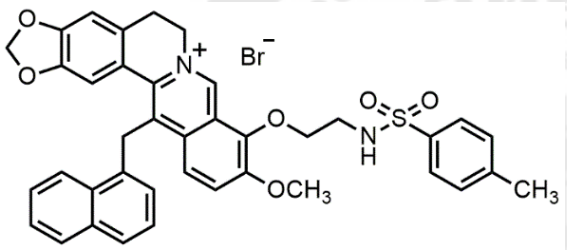

To a suspension of the *p*-toluenebenzenesulfonyl chloride (500 mg, 2.62 mmol) in ethyl acetate (5 mL), 2-bromoethylamine hydrobromide (698.5 mg, 3.41 mmol) and triethylamine (0.73 mL, 5.25 mmol) were added at 0 °C. The mixture was then stirred at room temperature for 4 h, then concentrated under reduced pressure. The crude product was purified by column chromatographed on silica gel (50%Hexane/DCM) to give the intermediate reagent. A mixture of compound **12** (100.6 mg, 0.20 mmol) and anhydrous potassium carbonate (K_2CO_3) (27.8 mg, 0.20 mmol) was added to anhydrous acetonitrile (10 mL). The resulting red suspension was stirred in an oil bath, followed by adding the intermediate reagent (167.75 mg, 0.60 mmol). The reaction mixture was refluxed at 80 °C for 4 days. The mixture color was changed to yellow and monitored by TLC analysis. Subsequently, the mixture was then concentrated under reduced pressure and chromatographed on silica column (2% MeOH/DCM) to give **21** (3.9 mg, 2.6 %) as a yellow solid. ^{1}H NMR ($CDCl^3$, 500 MHz): δ 10.92 (s, 1H, 8-H), 8.58 (t, 1H, *J* = 5.5 Hz, N-H), 7.55 (d, 1H, *J* = 9.5 Hz, 11-H), 7.46 (d, 1H, *J* = 9.5 Hz, 12-H), 7.40 - 8.10 (d, 4H, *J* = 8 Hz, benzene Ar-H), 6.93 (s, 1H, 1-H), 6.85 (s, 1H, 4-H), 6.8-8.2 (m, 7H, naphthyl Ar-H),

5.87 (s, 2H , OCH_2O), 5.31 (brs, 2H, 6-H), 5.00 (s, 2H, CH_2-Ar), 4.65 (t, 2H, *J* = 5 Hz, 9-OCH_2), 3.94 (s, 3H, 10-OCH_3), 3.42(d, 2H, *J* = 4 Hz, OCH_2CH_2NH), 3.28 (brs, 2H, 5-H), 2.38(s,3H, CH_3-benzene). HRMS (ESI): m/z calcd for C39H35N2O6S [M]+: 659.2210; found: 659.2200.

Synthesis of compound 24

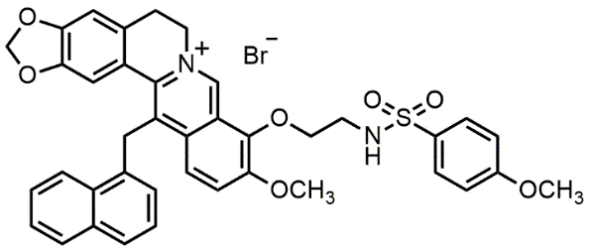

To a suspension of the 4-methoxybenzenesulfonyl chloride (500 mg, 2.42 mmol) in ethyl acetate (5 mL), 2-bromoethylamine hydrobromide (644.5 mg, 3.15 mmol) and triethylamine (0.67 mL, 4.84 mmol) were added at 0 °C. The mixture was then stirred at room temperature for 4 h, then concentrated under reduced pressure. The crude product was purified by column chromatographed on silica gel (60%Hexane/DCM) to give the intermediate reagent. A mixture of compound **12** (56.4 mg, 0.11 mmol) and anhydrous potassium carbonate (K_2CO_3) (15.7 mg, 0.11 mmol) was added to anhydrous acetonitrile (15 mL). The resulting red suspension was stirred in a sealed tube, followed by adding the intermediate reagent (100 mg, 0.34 mmol). The reaction mixture was refluxed at 80 °C for 4 days. The mixture color was changed to yellow and monitored by TLC analysis. Subsequently, the mixture was then concentrated under reduced pressure and chromatographed on silica column (2.5% MeOH/DCM) to give **24** (20 mg, 23.4%) as a yellow solid. ^{1}H NMR ($CDCl_3$, 500 MHz): **δ** 10.89 (s, 1H, 8-H), 8.52 (t, 1H, *J* = 5 Hz, N-H), 7.55 (d, 1H, *J* = 9.5 Hz, 11-H), 7.46 (d, 1H, *J* = 9.5 Hz, 12-H), 6.93 (s, 1H, 1-H), 6.90 - 8.20 (m, 7H, naphthyl Ar-H), 6.90 - 8.00 (d,4H, *J* = 8.5 Hz, benzene Ar-H), 6.85 (s, 1H, 4-H), 5.87 (s, 2H , OCH_2O), 5.28 (brs, 2H, 6-H), 5.00 (s, 2H, CH_2-Ar), 4.65 (brs, 2H, 9-OCH_2), 3.94 (s, 3H, 10-OCH_3), 3.83 (s, 3H, OCH_3-benzene), 3.40 (d, 2H, *J* = 3 Hz, OCH_2CH_2NH), 3.28 (brs, 2H, 5-H). HRMS (ESI): m/z calcd for $C_{39}H_{35}N_2O_7S$ $[M]^+$: 675.2159; found: 675.2158.

Synthesis of compound 27

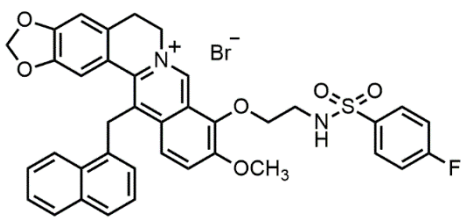

To a suspension of the 4-fluorobenzenesulfonyl chloride (500 mg, 2.57 mmol) in ethyl acetate (5 mL), 2-bromoethylamine hydrobromide (684 mg, 3.34 mmol) and triethylamine (0.72 mL, 5.14 mmol) were added at 0 °C. The mixture was then stirred at room temperature for 4 h, then concentrated under reduced pressure. The crude product was purified by column chromatographed on silica gel (DCM) to give the intermediate reagent. A mixture of compound **12** (50 mg, 0.11 mmol) and anhydrous potassium carbonate (K_2CO_3) (29.9 mg, 0.22 mmol) was added to anhydrous acetonitrile (10 mL). The resulting red suspension was stirred in a sealed tube, followed by adding the intermediate reagent (91.5 mg, 0.32 mmol). The reaction mixture was refluxed at 80 °C for 4 days. The mixture color was changed to yellow and monitored by TLC analysis. Subsequently, the mixture was then concentrated under reduced pressure and chromatographed on silica column (2.5% MeOH/DCM) to give **27** (25 mg, 28.6%) as a yellow solid. ^{1}H NMR ($CDCl_3$, 500 MHz): δ 10.86 (s, 1H, 8-H), 8.82 (brs, 1H, N-H), 7.08-7.93 (d, 2H, *J* = 8 Hz, benzene Ar-H), 7.57 (d, 2H, *J* = 9.5 Hz, 12-H), 7.48 (d, 2H, *J* = 9.5 Hz, 11-H), 6.89 (s, 1H, 1-H), 6.85 (s, 1H, 4-H), 6.8-8.2 (m, 7H, naphthyl Ar-H), 5.86 (s, 2H , OCH_2O), 5.28 (brs, 2H, 6-H), 5.00 (s, 2H, CH_2- Ar), 4.66 (brs , 2H , 9-OCH_2), 3.95 (s, 3H, 10-OCH_3), 3.43 (brs , 2H , 9-OCH_2CH_2NH), 3.24 (brs, 2H, 5-H). HRMS (ESI): m/z calcd for $C_{39}H_{32}FN_2O_6S$ $[M]^+$: 663.1960; found: 663.1989.

Synthesis of compound 30

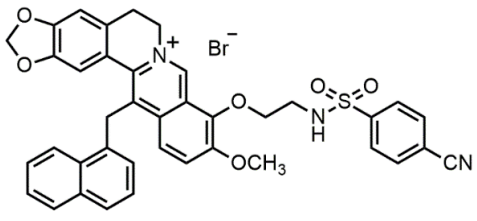

To a suspension of the 4-cyanobenzenesulfonyl Chloride (500 mg, 2.48 mmol) in ethyl acetate (5 mL), 2-bromoethylamine hydrobromide (660.5 mg, 3.22 mmol) and triethylamine (0.69 mL, 4.96 mmol) were added at 0 °C. The mixture was then stirred at room temperature for 4 h, then concentrated under reduced pressure. The crude product was purified by column chromatographed on silica gel (50%Hexane/DCM) to give

the intermediate reagent. A mixture of compound **12** (50 mg, 0.11 mmol) and anhydrous potassium carbonate (K_2CO_3) (29.9 mg, 0.22 mmol) was added to anhydrous acetonitrile (10 mL). The resulting red suspension was stirred in a sealed tube, followed by adding the intermediate reagent (93.8 mg, 0.32 mmol). The reaction mixture was refluxed at 80 °C for four days. The mixture color was changed to yellow and monitored by TLC analysis. Subsequently, the mixture was then concentrated under reduced pressure and chromatographed the designed products on silica gel (2.5% MeOH/DCM) to give **30** (49 mg, 65 %) as a yellow solid. ^{1}H NMR ($CDCl_3$, 500 MHz): δ 10.80 (s, 1H, 8-H), 9.14 (brs, 1H, N-H), 7.76 -8.20 (d, 4H, *J* = 8.5 Hz, benzene Ar-H), 7.56 (d, 2H, *J* = 9.5 Hz, 11-H), 7.49 (d, 2H, *J* = 9.5 Hz, 12-H), 6.87 (s, 1H, 1-H), 6.84-8.13 (m, 7H, naphthyl Ar-H), 6.84 (s, 1H, 4-H), 5.87 (s, 2H , OCH_2O), 5.29 (brs, 2H, 6-H), 5.00 (s, 2H, CH_2-Ar), 4.65 (t , 2H, *J* = 4.5 Hz, 9-OCH_2), 3.96 (s, 3H, 10-OCH_3), 3.45 (brs , 2H, *J* = 5 Hz, 9-$OCH_2C\mathbf{H}_2NH$), 3.26 (brs, 2H, 5-H). HRMS (ESI): m/z calcd for $C_{39}H_{32}N_3O_6S$ $[M]^+$: 670.2006; found: 670.2002.

Synthesis of compound 33

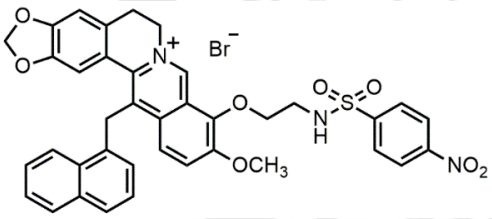

To a suspension of the 4-nitrobenzenesulfonyl chloride (500 mg, 2.26 mmol) in ethyl acetate (5 mL), 2-bromoethylamine hydrobromide (603 mg, 2.94 mmol) and triethylamine (0.63 mL, 4.53 mmol) were added at 0 °C. The mixture was then stirred at room temperature for 4 h, then concentrated under reduced pressure. The crude product was purified by column chromatographed on silica gel (50%Hexane/DCM) to give the intermediate reagent. A mixture of compound **12** (50 mg, 0.11 mmol) and anhydrous potassium carbonate (K_2CO_3) (29.9 mg, 0.22 mmol) was added to anhydrous acetonitrile (10 mL). The resulting red suspension was stirred in a sealed tube, followed by adding the intermediate reagent (100.3 mg, 0.32 mmol). The reaction mixture was refluxed at 80 °C for four days. The mixture color was changed to yellow and monitored by TLC analysis. Subsequently, the crude product was then concentrated under reduced pressure and chromatographed on silica column (2.5% MeOH/DCM) to give **33** (16 mg, 33.9%) as a yellow solid. ^{1}H NMR ($CDCl_3$, 500 MHz): δ

10.82 (s, 1H, 8-H), 8.50 (s, 1H, N-H), 8.1-8.32 (d, 4H, *J* = 8.5 Hz, benzene Ar-H), 7.58 (d, 2H, *J* = 9.5 Hz, 11-H), 7.49 (d, 2H, *J* = 9 Hz, 12-H), 6.93 (s, 1H, 1-H), 6.85-8.63 (m, 7H, naphthyl Ar-H), 6.84 (s, 1H, 4-H), 5.87 (s, 2H, OCH_2O), 5.28 (brs, 2H, 6-H), 5.01 (s, 2H, CH_2- Ar), 4.66 (t, 2H, *J* = 4.5 Hz, 9-OCH_2), 3.98 (s, 3H, 10-OCH_3), 3.47 (d, 2H, *J* = 4.0 Hz, 9-OCH_2CH_2NH), 3.23 (brs, 2H, 5-H). HRMS (ESI): m/z caled for $C_{38}H_{32}N_3O_8S$ $[M]^+$: 690.1905; found: 690.1887.

Bioactivity evaluation

Cell cultures and cell viability assay

HepG2 cells were cultured in RPMI 1640 Medium (Roswell Park Memorial Institute 1640 Medium) with 10% fetal bovine serum (FBRS; Gibco, Grand Island, NY, USA) and 100 U/mL streptomycin-penicillin solutions. The cells were maintained in a humidified 5% CO_2 incubator at 37 °C. The MTT assay was used to indicate cell viability. First, the HepG2 cells were seeded 2 x 10^4 cells/well in a 96-well plate in an incubator with 5% CO_2 at 37 °C overnight. Then, cells were incubated with MTT reagent (100 μL/well of 5 mg/mL) for 4 hours after being treated with BBR and its derivatives at various concentrations for 24 h. Finally, the medium was removed and the purple formazan crystals was dissolved in DMSO (100 μL/well). The absorbance was measured at 595 nm.

PCSK9 Elisa assay

The commercially available PCSK9 assay kit, The LEGEND MAX™ Human PCSK9 ELISA Kit, from BioLegend, Catalog Number 443107, was used to evaluate the PCSK9 inhibition following the manufacturer's instructions. Briefly, HepG2 Cells were seeded for 10 x 10^4 cells/well in a 48-well plate then incubated at 37°C in an incubator with 5% CO_2 overnight. Then, cells were treated with BBR and BBR derivatives at various concentrations for 24 h. The culture medium was collected to a 1.5 mL centrifuge tube and centrifuged to remove cell debris at 10,000 rpm for 2 min, respectively. The human PCSK9 standard were prepared at 30, 15, 7.5, 3.75, 1.88, 0.94, 0.47 ng/mL and Assay Diluent D serves as the zero standards (0 ng/mL). The plate was washed four times, then add 50 μL of Assay Buffer A to each well. Afterwards, 50 μL of prepared standard dilutions or samples were added into the pre-coated well for 2 h incubation while shaking at higher

than 200 rpm. Each well was washed four times, then an hour co-incubated with 100 µL of Human PCSK9 Detection Antibody solution at room temperature while shaking. For the PCSK9 quantification, 100 µL of Avidin-HRP solution was added to each well while shaking for 30 min. Each well was washed four times. Then, wells containing human PCSK9 should turn blue with intensity proportional to concentration after added 100 µL of substrate Solution F and incubated for 15 minutes in the dark. Finally, each well was washed six times and added 100 µL of the stop solution, the color should change from blue to yellow and record the OD at 450 nm to analyze the results.

Statistical analysis

All experiments were performed in triplicate (n=3), and data were presented as mean ± standard deviation (SD). The 50% inhibitory concentration (IC_{50}) was calculated by using the GraphPad Prism 3.03 software (GraphPad Software, Inc., San Diego, CA, USA).

CHAPTER 4
RESULTS

Molecular docking of PCSK9

AutoDock approach was applied to study the binding affinities of BBR and its derivatives to PCSK9 proteins to obtain the novel small molecule as PCSK9 inhibitors. Previously, Cameron et al. studied the effect of BBR on the amount of PCSK9 and LDLR mRNA. The results suggested that BBR decreased PCSK9 mRNA and increased LDLR mRNA (Cameron et al., 2008). However, based on the SARs study, the quaternary ammonium cation of BBR results in its poor aqueous solubility properties (Gaba et al., 2021). As a result, absorption of the gastrointestinal tract was decreased, which was a severe limitation as a pharmaceutical preparation. Therefore, the structure of BBR was modified on several positions, which led to synthesis of various BBR derivatives to improve the therapeutic potential and combat pharmacokinetic limitations. The positions of the BBR scaffold were generally introduced at the C-2, C-3, C-8, C-9, C-10, C-12, and C-13 in structural modifications (Patel, 2021) (Figure 16).

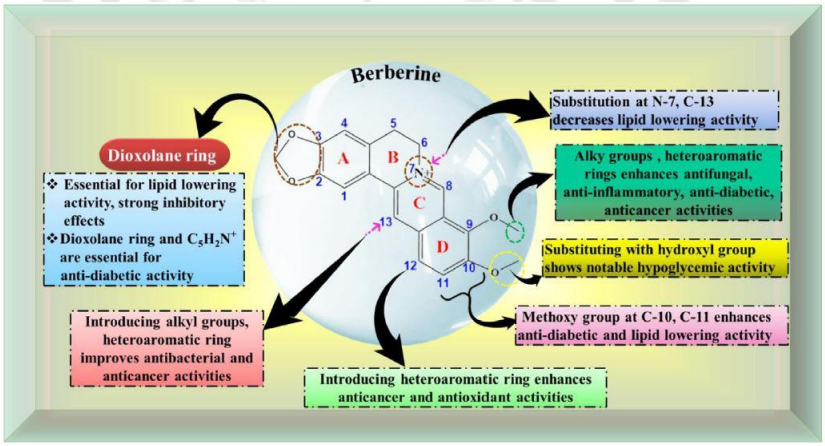

Figure 16 Structure modification of BBR at various position.

Source: Patel, P. (2021). A bird's eye view on a therapeutically 'wonder molecule': Berberine. *Phytomedicine Plus,* 1(3), 100070.

In 2018, BBR derivatives were introduced naphthalenylmethyl moiety at position C-13 and substituted with alkoxy carboxylic acid at the C-9 position. The result showed that all derivatives could inhibit HMGCR activity. Especially, compounds **34** and **35** (Figure 17) displayed a high inhibitory effect on HMGCR by 12-fold higher activity than BBR. In addition, they showed stronger binding interaction with PMK at K_d values of 64.77 ± 4.80 and 85.09 ± 6.84 μM, respectively (Jaitrong, 2018).

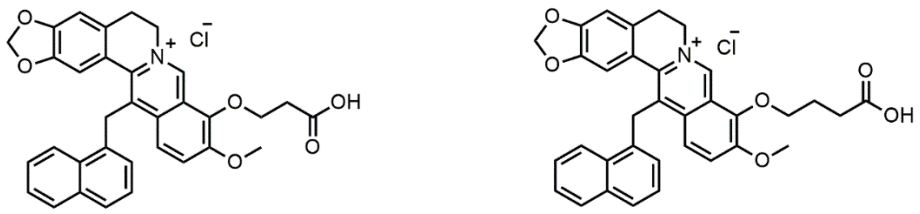

Figure 17 Structures of compounds **34** and **35**

Fortunately, our in-house BBR derivatives library, compound **2** was represented series of BBR derivatives with anti-hyperlipidemic activity through HMGCR inhibition (Jaitrong, 2018). Compound **2** was introduced with the naphthalennylmethyl moiety, which contains in statin structure at the C-13 of the aromatic ring C of the BBR scaffold, to increase lipophilicity and then was screened to inhibit PCSK9 expression. The obtained result showed better binding energy (-6.84 kcal/mol), which is stronger than the parent BBR (-5.08 kcal/mol). In addition, the naphthalenylmethyl moiety increased three hydrophobic interactions, especially with Ile369, which play an important role in the PCSK9 interface (Xu et al., 2019), as shown in Figure 18.

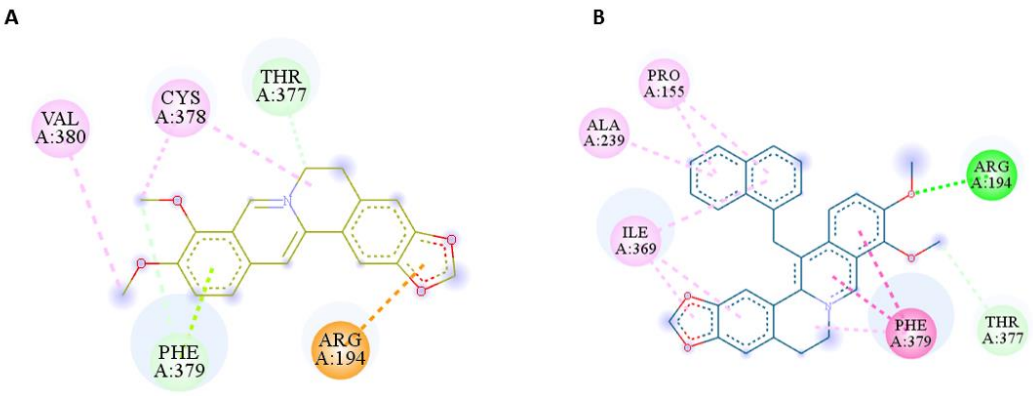

Figure 18 The 2D interactions of BBR (A) and compound **2** (B) with PCSK9.

In addition, BBR has also been reported that the C-9 position could essentially enhance cholesterol-lowering activity by introducing long-chain alkyl groups (Figure 20)(D. D. Li et al., 2021). The obtained result showed that compound **36** exhibited the most inhibitory activity of the total cholesterol (TCHO) levels expression in HepG2 cells. In comparison, compound **37** inhibited the expression of triglyceride, that the inhibition rate was nearly 70%. As well as, the LDL-C level improvement was significantly reduced by introducing the fibrates at the C-9 position (**38**). In addition, the reduction of the N-7 position (**39**) was a good performance in terms of HDL-C increasing.

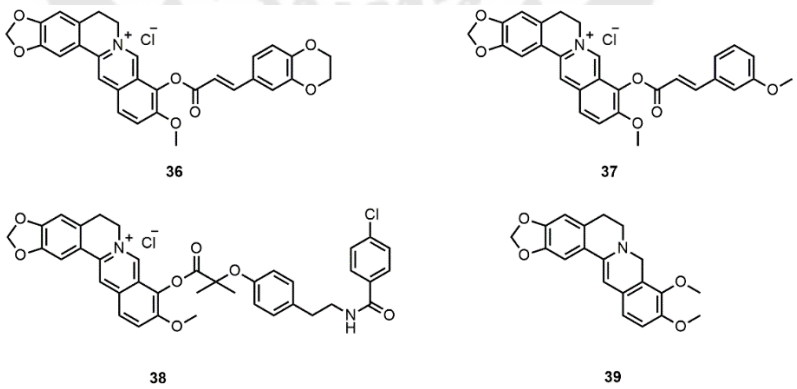

Figure 19 Structures of the BBR derivatives (the C-9 modification) as novel lipid-lowering agents.

Interestingly, the sulfonamide alkyl linker was introduced to the morpholine (**8**) (Chapter 2, Section PCSK9 inhibitor), which showed very promising for the PCSK9

modulation activity with EC_{50} values less than 1 nM (Xie et al., 2020). Furthermore, the fluorobenzenesulfonate derivative of corydaline increased hepatic LDLR expression and downregulated PCSK9 expression (Xu et al., 2019). On top of that, a novel series of naphthalenylmethyl-containing BBR derivatives were designed based on the core of structure **2**. The designed series of BBR derivatives **13-18**, which a long alkyl chain branched (n = 1-6) with the benzenesulfonyl group at the 9-position, was shown in Table 1. The results revealed that the predicted binding energy of alkoxy benzenesulfonamide derivatives increased with the length of aliphatic chain elongation were more potent than **2**. Among them, compound **14** overlaid on the PCSK9 similar to BBR and showed the lowest binding energy (-7.92 Kcal/mol), as shown in Figure 20.

Table 1 Binding energy of berberine and its derivatives to PCSK9 were obtained from molecular docking studies.

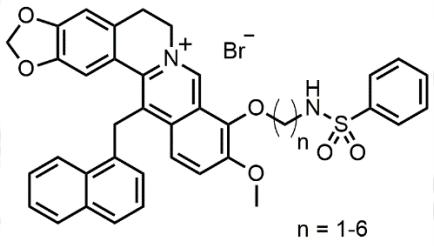

Compound	n	Binding energy (kcal/mol)
BBR (1)	-	-5.08
2	-	-6.38
12	-	-6.48
13	1	-7.51
14	2	-7.92
15	3	-7.39
16	4	-6.71
17	5	-6.97
18	6	-6.75

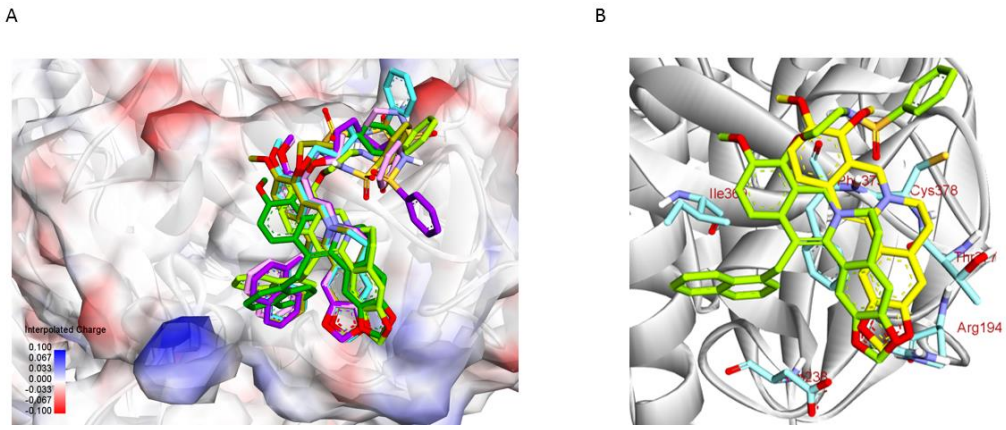

Figure 20 Superimposed of Berberine derivatives: (A) an alkoxy benzenesulfonamide derivatives increased with the length of aliphatic chain elongation (n=1-6); (B) Compound **14** (light green), BBR (yellow), and key residues (cyan) overlaid on the prodomain of PCSK9.

Compound **14** with the lowest binding energy was selected to study the substitution effect on the benzenesulfonyl group. Additionally, compounds **19-33** were explored to improve the binding affinity by bearing CH_3, OCH_3, F, CN, or NO_2 group at the ortho-, *meta*-, and *para*- positions of benzenesulfonyl ring. The results showed that all compounds possessed a binding affinity at -6.74 to -8.15 kcal/mol, better than that of BBR (-5.08 kcal/mol). The effect of an electron-donating/withdrawing group substitution on the benzenesulfonyl ring at the *ortho*-, *meta*-, *para*- position were no significantly different in binding energy as shown in Table 2.

Table 2 Substituent effects on the binding energies of benzenesulfonamide derivatives **19-33** to PCSK9.

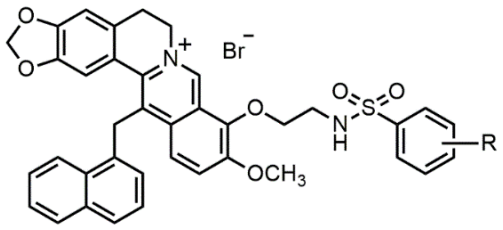

Compound	R	Binding energy (kcal/mol)
19	2-CH_3	-7.49
20	3-CH_3	-7.92
21	4-CH_3	-6.90
22	2-OCH_3	-6.74
23	3-OCH_3	-7.14
24	4-OCH_3	-6.88
25	2-F	-7.29
26	3-F	-8.15
27	4-F	-6.55
28	2-CN	-7.07
29	3-CN	-7.38
30	4-CN	-6.84
31	2-NO_2	-6.94
32	3-NO_2	-6.86
33	4-NO_2	-7.56

Besides, the key interactions of PCSK9 with EGF(A) are formed between residues 377-379 and 308-310, respectively. In addition, other residues of PCSK9, including Arg194, Asp238, Ile369, are crucial for the binding. Then, the designed molecules that mimic EGF(A) interface regions bound to PCSK9 would be the good candidate for further drug development. The obtained result showed that all designed compounds interacted with Arg194, Phe379 residues via hydrogen bonds and hydrophobic interactions, while the hydrophobic interaction favorable formed with Ile369 residue. Surprisingly, most of the compounds which substituted at the *para*-direction

interacted with key residue Thr377 via Pi-lone pair interactions, except compound **21**. Therefore, the designed BBR derivatives that substituted benzenesulfonamide at the *para*-direction were identified as the most potent inhibitors due to similar interactions with EGF(A) compared to other positions (Table 3). The structure of selected compounds were shown in Figure 21.

Table 3 Interactions of PCSK9 amino acid residues with BBR derivatives at other positions.

Compound	R	Amino acid involved (distance in **Å**)*			
		Hydrogen bond	Hydrophobic interaction	Electrostatic interaction	Other
19	2-CH_3	Arg194 (2.06, 3.15, 3.91), Phe379 (2.02)	Ile369 (3.84, 4.74), Phe379 (4.43, 4.56, 4.87, 5.39), Val380	Arg194 (3.15, 3.91)	-
20	3-CH_3	Arg194 (3.26), Phe379 (1.89, 2.19, 3.48)	Ile369 (3.84, 4.58, 5.18, 5.25), Phe379 (4.50, 4.77, 4.80), Val380	Arg194 (3.26), Asp374 (3.26)	Phe379 (2.42)
21	4-CH_3	Phe379 (1.87, 2.15, 3.44)	Pro155, Ala239, Ile369 (4.30, 5.04), Cys378 (5.03), Phe379 (5.31, 5.42, 5.59), Val380	-	-
22	2-OCH_3	Phe379 (2.17, 2.39, 2.66, 3.62), Ser381 (3.43)	Ile369 (4.33, 4.96, 5.39), Phe379 (5.42)	-	Cys375 (4.36)

* The distances were presented when BBR derivatives interacted with key residues of PCSK9.

Table 3 (continued)

Compound	R	Amino acid involved (distance in **Å**)*			
		Hydrogen bond	Hydrophobic interaction	Electrostatic interaction	Other
23	3-OCH_3	Arg194 (2.49, 3.22), Phe379 (2.11, 2.94)	Ile369 (3.95, 4.06, 4.46, 4.90), Phe379 (4.55, 4.71, 4.73, 4.85, 5.64), Val380	Arg194 (3.22)	Phe379 (2.89)
24	4-OCH_3	Arg194 (3.28), Thr377(3.26), Phe379 (2.14, 2.73)	Pro155, Ile369 (3.92, 4.71, 5.15, 5.35), Phe379 (3.47, 4.95, 5.39), Val380	Arg194 (3.28)	Cys375, Phe379 (2.06, 2.33)
25	2-F	Phe379 (2.21, 3.30, 3.71)	Ile369 (3.56, 3.83), Phe379 (4.49, 4.63, 4.74), Val380	-	-
26	3-F	Arg194 (2.22, 3.08, 4.09), Phe379 (1.92, 2.00, 3.73)	Ile369 (3.87, 3.89, 4.90), Phe379 (4.56, 4.64, 4.72, 5.06), Val380	Arg194 (3.08, 4.09)	-
27	4-F	Thr377 (3.48), Phe379 (1.54, 2.27, 3.56)	Pro155, Ala239, Ile369 (4.42, 4.96, 5.41), Phe379 (3.75, 5.16, 5.26), Val380	-	Phe379 (2.81)
28	2-CN	Phe379 (1.95, 2.50, 2.90)	Ile369 (3.43, 3.51, 3.54, 3.69, 4.64), Phe379 (3.43, 4.67, 5.03, 5.37), Val380	-	-

* The distances were presented when BBR derivatives interacted with key residues of PCSK9.

Table 3 (continued)

Compound	R	Amino acid involved (distance in Å)*			
		Hydrogen bond	Hydrophobic interaction	Electrostatic interaction	Other
29	3-CN	Arg194 (1.78, 3.53), Phe379 (2.41)	Pro155, Ala239, Ile369 (3.95, 4.18, 4.82), Phe379 (3.54), Val380	Arg194 (3.53)	-
30	4-CN	Arg194 (2.02, 2.66)	Pro155, Ala239, Ile369 (3.77, 3.88, 5.26, 5.40), Phe379 (5.05, 5.97), Val380	-	Thr377 (2.83)
31	2-NO_2	Cys375 (3.45, 3.74)	Ile369 (4.04, 4.45, 4.70), Phe379 (4.25, 4.30, 5.47, 5.85)	-	-
32	3-NO_2	Arg194 (1.85, 2.22, 2.89), Phe379 (3.45)	Ile369 (3.95, 5.24, 5.44), Phe379 (4.02, 5.55, 5.76, 5.89), Val380	-	-
33	4-NO_2	Arg194 (1.70, 1.91), Phe379 (1.95, 3.11)	Pro155, Ala239, Ile369 (4.99, 5.32), Phe379 (5.15, 5.92, 5.97), Val380	Arg194 (4.14)	Thr377 (2.18)

* The distances were presented when BBR derivatives interacted with key residues of PCSK9.

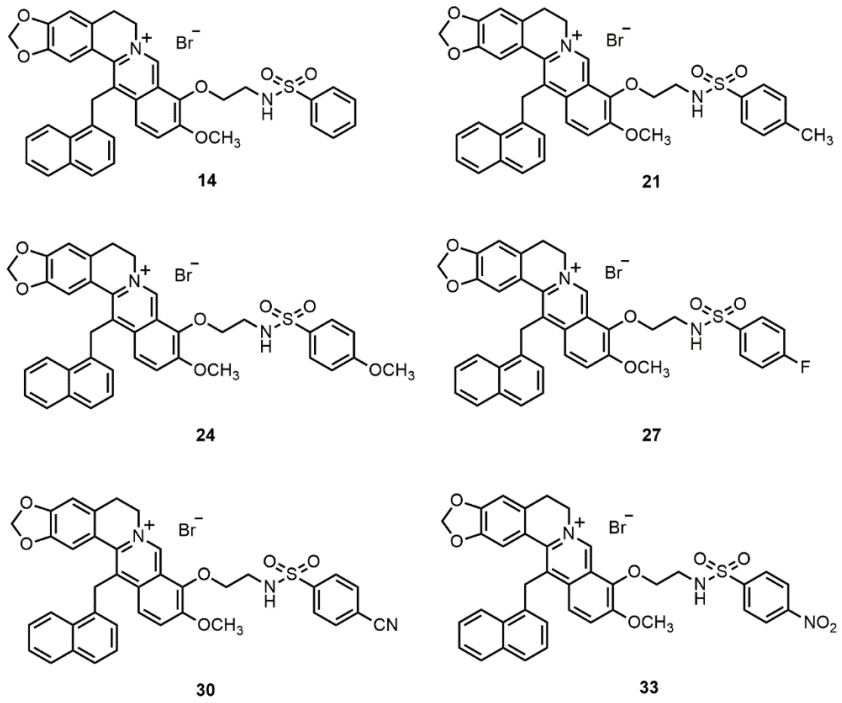

Figure 21 Structures of the selected designed BBR derivatives.

Drug likeness

The observation of the most biologically active drugs was evaluated by Lipinski's rule that describes absorption and permeation of a drug on oral activity for initial screening of drug-likeness. Five criteria of Lipinski's rule consist of MW of approximately 500 Da; the results presented in Table 4 indicated that all the compounds analyzed have MW>500. Thus, they have poor drug distribution. The lipophilicity properties confirmed by miLogP is approximately 0.4 to 5; the obtained results showed that all the compounds met this criteria. The characterization of drug absorption, including intestinal absorption and penetration of the blood-brain barrier (BBB), are described with TPSA and nRB. The designed compounds showed TPSA <140 $Å^2$ and nRB <10. In addition, total hydrogen counts (HBD and HBA) are perfect predictors of good oral bioavailability, and most compounds passed the evaluation except compound **24**. Furthermore, the designed BBR derivatives fulfiled Lipinski's rule, which implies as a good oral bioavailability inhibitors.

Table 4 Physicochemical properties of sulfonamide derivatives **2**, **3**, **14**, **21**, **24**, **27**, **30**, **33** and **BBR**.

Compound	MW	miLogP	HBA	HBD	TPSA	nRB	nviolations**
2	476.55	3.24	5	0	40.82	4	0
3	462.52	2.97	5	1	51.81	3	0
14	645.76	3.94	8	1	86.99	9	1
21	663.75	4.10	8	1	86.99	9	1
24	690.75	3.90	11	1	132.81	10	2
27	670.77	3.69	9	1	110.78	9	1
30	659.78	4.39	8	1	86.99	9	1
33	675.78	3.99	9	1	96.22	10	1
BBR	336.37	0.20	5	0	40.82	2	0

*MW: Molecular Weight; miLogP: molinspiration Log partition coefficient; HBA: Hydrogen bond acceptor; HBD: Hydrogen bond donor; TPSA: topological polar surface area; nRB: number of rotatable bonds.

**number of violations $\leq$ 1 : acceptable drug-like properties.

Therefore, the core structure of BBR was modified at C-9 by introducing an alkoxy benzenesulfonamide which was substituted with an electron-donating/withdrawing group at the *para*-position of the benzene ring. In addition, the naphthalenylmethyl moiety was attached to C-13. Eventually, the desired BBR derivatives were synthesized based on the four-step strategy as described in the following sections.

Synthesis

On the basis of the above design, a series of BBR derivatives containing naphthalene moiety (**2**, **3**, **14**, **21**, **24**, **27**, **30**, **33**) was synthesized through the route as shown in Figure 18 (Chapter 3). Mannich reaction of BBR was performed to obtain the corresponding unstable 8-acetonyldihydroberberine (**11**), and subsequent alkylation with 1-(chloromethyl)naphthalene to give 13-(1-naphthalenylmethyl)berberine (**2**) Demethylation of the resulting **2** with DMF under high pressure produced the 13-(1-naphthalenylmethyl)berberrubine (**12**). In the presence of a base, compound **12** was

alkylated with a corresponding alkylating agent to afford the desired compounds in a good yield.

Mannich Reaction

8-Acetonyldihydroberberine (**11**) can be obtained by reaction of BBR with acetone in aqueous NaOH at 65°C, resulting in high yields of a pale yellow solid (85%). This compound was immediately alkylated in the next step without purification and characterization because it was an unstable product.

Enamine Alkylation

13-(1-naphthalenylmethyl)berberine (**2**) can be accessed by C-alkylation of **11** with 1-(chloromethyl)naphthalene at 80°C to generate **2** in moderate yield (51.3%). The NMR spectroscopic technique was used for analyzing the structure of **2**. The ^{1}H NMR revealed a signal assigned to the H-8 proton next to an iminium salt at δ 10.62 as a singlet, and the resumed of seven aromatic protons of the naphthyl group in the region of δ 7.27 – 8.10 appeared as multiplet. Moreover, none of the acetonyl group signals was observed.

Demethylation

13-(1-naphthalenylmethyl)berberrbine (**12**) can be achieved by heating in DMF at 150 °C in sealed tube. The resulting red solid of **12** was obtained in moderate yield (68.6%). The ^{1}H NMR of **12** showed a similar signal pattern to **2**. Additionally, the singlet signal integrating for three protons assigned to the methoxy group of C-9 around δ 4.37 was disappeared.

***O*-alkylation**

The 13-(1-naphthalenylmethyl)-9-alkoxy benzenesulfonamide derivatives can be afforded by alkylation of **12** with a corresponding alkylating agent in the presence of K_2CO_3 in a sealed tube. The yields were obtained in the range of 2.6-65 %.

The ^{1}H NMR of **14** showed similar signals to those of **12** with some extra signals of four aromatic protons at δ 7.28 and 7.90 assigned to the sulfonamide benzene ring and four methylene proton signals at δ 4.66 and 3.43 attributed to OCH_2 and NCH_2 groups, respectively. High-resolution mass spectral analysis (ESI) showed a positive at *m/z* 645.2022, corresponding to the formula of the cation **14**. The structure of **21** was

confirmed by ^{1}H NMR spectroscopic data and mass spectrometry. The ^{1}H NMR spectrum showed a triplet signal ascribed to the sulfonamide NH at δ 8.59. Two sets of doublet between δ 7.26-7.98, integrating for a total of 4 protons, were attributed to the aromatic protons of the benzene moiety. A signal attributed to two protons of OC**H**$_2$CH$_2$NH appeared at δ 4.66 and OCH$_2$C**H**$_2$NH at δ 3.41. A characteristic signal for benzene ring product at δ 2.38 as a singlet attributed to a methyl group which did not correlate with any nearby proton in the COSY spectrum. The HRMS (ESI) spectrum provided additional confirmation of the structure, which performed a molecular ion signal at *m/z* 659.2200, consistent with the molecular formula of **21**. The ^{1}H NMR spectrum of **24** was very similar to that of **21** except for the presence of a singlet signal at δ 3.83 integrating for three protons assigned to the methoxy protons. The HRMS (ESI) spectrum noticed that the peak corresponded to the molecular ion (*m/z* 675.2158) consistent with the molecular formula of **24**. All spectroscopic data of **27**, **30**, **33** were closely comparable to **14**, with a slight difference in extra integration of the signals attributed to the aromatic protons of the benzene moiety in a range of δ 7.60-8.50 and two sets of all other signals. In addition, a characteristic signal for benzene ring of **27** appeared as a triplet due to coupling between hydrogen and fluorine. The HRMS (ESI) spectrum showed a signal at *m/z* 663.1989 (compound **27**), 670.2002 (compound **30**), 690.1887 (compound **33**), respectively. The proposed mechanism of desired compounds was shown in Figure 22.

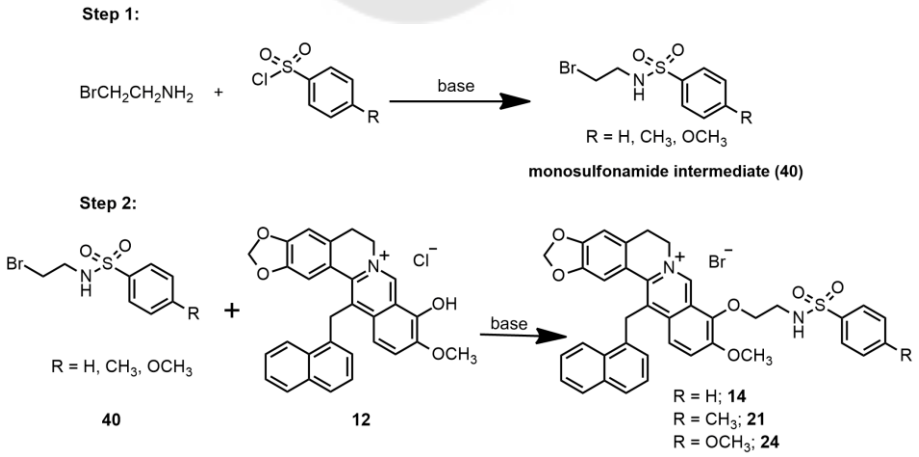

Figure 22 The proposed mechanism of desired compounds.

The addition of a *para* hydroxyl group will influence the electron density of the phenyl ring through its ability to interact with the aromatic electrons. In benzene moiety substituted with electron-withdrawing groups (**27**, **30**, **33**), product formation in *O*-alkylation has generated the mixture of mono, and di-sufonamide product which was not successful in the attempted purification. Since the substituent is an electron-withdrawing group, it decreases electron density of sulfonamide nitrogen through phenyl ring resulting in an increase of sulfonamide-NH acidity. Under the basic condition, the NH proton is easily deprotonated, and hence sulfonamide nitrogen would act as a more reactive nucleophile than phenolic oxygen of compound **12**. Therefore, the nitrogen nucleophile attacked another molecule of monosulfonamide intermediate (**40**) to generate a disulfonamide agent (**41**). Then, both intermediates **40** and **41** reacted with **12** to give the desired compounds **27**, **30**, **33** and unexpected disulfonamide derivatives (**42-44**). The proposed mechanism was presented in Figure 23.

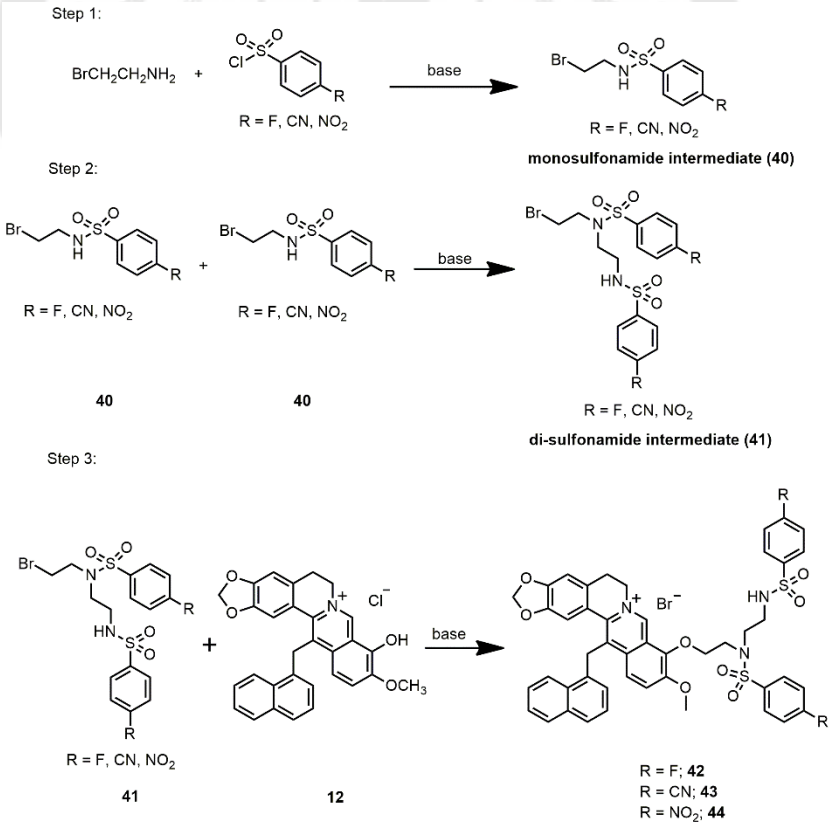

Figure 23 The proposed mechanism of unexpected products.

Inhibition activity of BBR derivatives against PCSK9

The PCSK9 expression was investigated on the HepG2 cells. Initial screening, the toxicity of each compound was carried out at various concentrations using MTT assay. The calculating $IC_{50}$of cytotoxicity of BBR and **12** in HepG2 cells showed no significant cytotoxicity (100 μmol/mL). In contrast, compounds **2**, **14**, **21**, and **24** showed cytotoxicity against HepG2 cells with IC_{50} less than 20 μmol/L, as shown in Tables 5 and 6.

Table 5 Cytotoxicity of Compounds **2**, **12**, and BBR in HepG2 cells.

Compound	Cell viability (% compared to control, mean±SD) at 100 μmol/L
2	2.68 ± 0.1
12	86.08 ± 2.7
BBR	72.92 ± 2.4
Control	95.27 ± 0.4

Table 6 Cytotoxicity of Compounds **14**, **21**, and **24** in HepG2 cells.

Compound	Cell viability (% compared to control, mean±SD) at 5 μmol/L
14	82.77 ± 3.3
21	73.34 ± 2.5
24	87.93 ± 1.0
Control	95.27 ± 0.4

Then, BBR derivatives with a concentration that gave the percentage of cell viability approximately 80 were examined for their ability to inhibit PCSK9 expression. The efficacy data showed that BBR (100 μmol/L) secreted PCSK9 protein by 21.7% compared to control. Firstly, the SARs study was focused on the effect of naphthalene moiety at the 13-position. To begin with, compound **2** showed significant cytotoxicity in HepG2 cells. Then, the methoxy group of **2** was demethylated at the 9-position. The obtained compound **12**

showed less PCSK9 expression activity than BBR at 100 μmol/L (43.17%) (Table 7). In addition, compounds **14** was investigated the side chain effect at the 9-position bearing alkoxy benzenesulfonamide. The result showed that compound **14** increased activity on the PCSK9 up-regulation (28.29%). Next, studies on the effect of substituents on the benzenesulfonamide ring of compound **14**, the hydrogen atom at the *para*-position on the benzene ring, was substituted with an electron-donating group. Compounds **21** and **24** exhibited significantly higher PCSK9 inhibition activity with 19.8 and 18.1% relative secreted PCSK9, respectively, which could be attributed to the influence of electronic donating groups (Table 8).

Table 7 Effects of compound **12** compared to BBR at 100 μmol/L on PCSK9 expression in HepG2 cells.

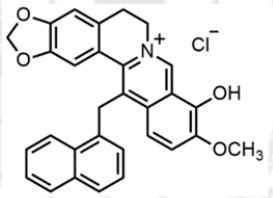

12

Compound (100 μmol/L)	Relative Percentage of Secreted Human PCSK9 (% of control)
12	43.17 ± 2.1
BBR	18.35 ± 1.4
Control	100.00 ± 2.4

Table 8 Effects of compounds **14**, **21**, and **24** at 5 μmol/L on PCSK9 expression in HepG2 cells.

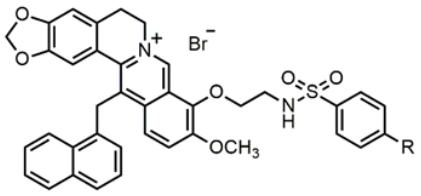

R = H, CH_3, OCH_3

Compound (5 μmol/L)	R	Relative Percentage of Secreted Human PCSK9 (% of control)
14	-H	28.29 ± 1.1
21	$-CH_3$	19.79 ± 0.7
24	$-OCH_3$	18.10 ± 0.9
Control	-	100.00 ± 2.4

Potential PCSK9 inhibitor for lipid reduction

A new potential target for anti-hypercholesterolemia is PCSK9 protein that plays an essential role in LDL-C metabolism by up-regulated degradation of LDLRs. Therefore, the inhibition of PCSK9 allowed elevating LDLR levels in the liver, resulting in more effective LDL-C destruction from blood circulation and a significant LDL-C reduction. However, the small molecule is a great challenge for PCSK9 inhibitor development based on cost and oral administration effectiveness. BBR is a natural product that displayed anti-hypercholesterolemic activity. The previous study reported that BBR (10 μmol/L) secreted PCSK9 protein by approximately 20% after simvastatin treatment (Song et al., 2018). Therefore, a novel series of BBR derivatives were designed, synthesized, and evaluated PCSK9 inhibition activity. Compounds **21** and **24** at 5 μmol/L reduced the PCSK9 protein expression similar to BBR at 100 μmol/L. The result indicated that the selected compounds (**21**, **24**) decreased PCSK9 secretion better than BBR about 20-fold (5 μmol/L). Taking into account, molecular docking was applied to investigate the mode of binding and their interactions. The results demonstrated that three modes of

binding were observed, including BBR pattern (**14**, **24**), compound **12**, and **21**, as shown in Figure 24.

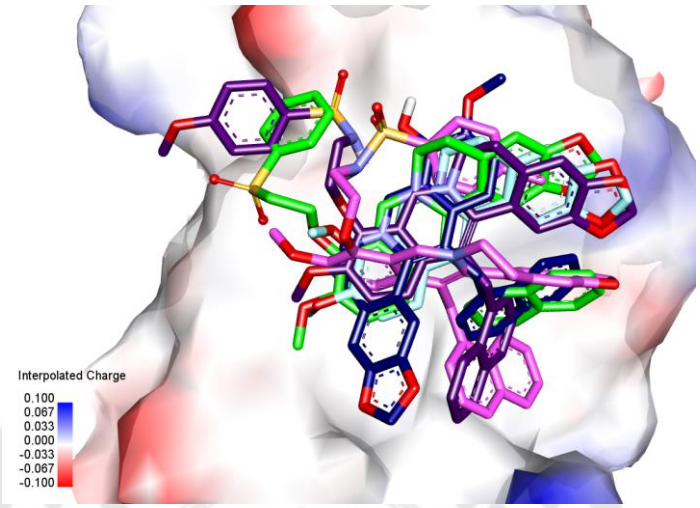

Figure 24 Superimposed of compounds **12** (navy blue), **14** (green), **21** (pink), **24** (purple) and BBR (cyan).

Compounds **14** and **24** posed in the binding pocket similar to BBR, as shown in Figure 25. In addition, a comparison of binding mode between BBR (Figure 18) and compounds **14** (Figure 25), **24** (Figure 26) found that 1, 3-Dioxolane of BBR core structure of those compounds generated electrostatic interaction with Arg194 whereas residue Thr377 interacted through a carbon hydrogen bond with C-6 of the compound. Additionally, amino acid Cys378 formed a hydrophobic interaction with OCH_3 of BBR and the benzene ring of compound **14**. Besides, sulfonyl moiety of **24** also interacted Cys378 via hydrogen bond. Moreover, the hydrogen bonds were observed between of ring C and OCH_3 of BBR to Phe379. In addition, two bonding of Phe379 residue occurred at rings A, C (hydrophobic interaction), and two hydrogen bonds formed to the sulfonamide group likewise compound **14**. In addition, a naphthalene moiety of **14** also generated hydrophobic interaction with Phe379. Furthermore, Val380 interacted with two hydrophobic interactions with *para*-methoxybenzene of compound **14** and formed to OCH_3 of BBR. Surprisingly, compound **24** showed the best potential PCSK9 inhibition

activity. Becaude of three hydrophobic interactions were generated between OCH_3 of C-10, ring D, and naphthalene moiety of compound **24**.

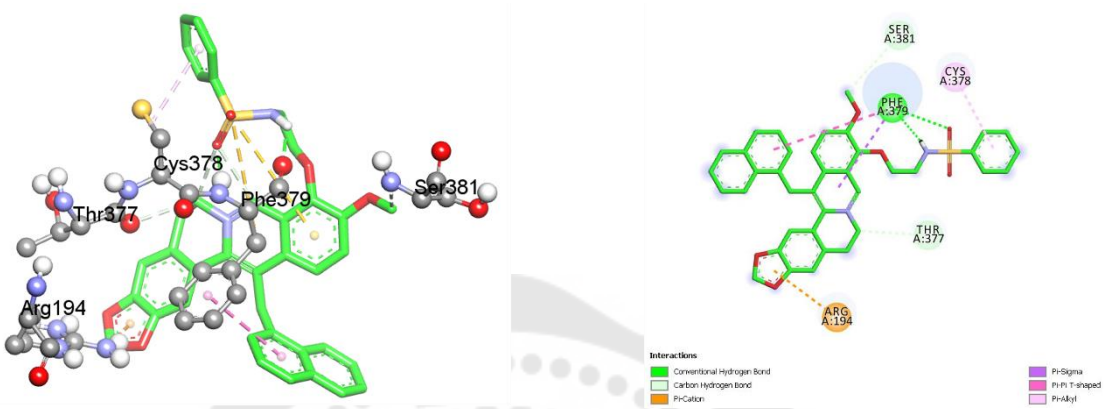

Figure 25 (A) Illustrates the 3D interactions of the best docking pose (compound **14**) on the surface of PCSK9 (B) 2D diagram of compound **14** interacted to PCSK9.

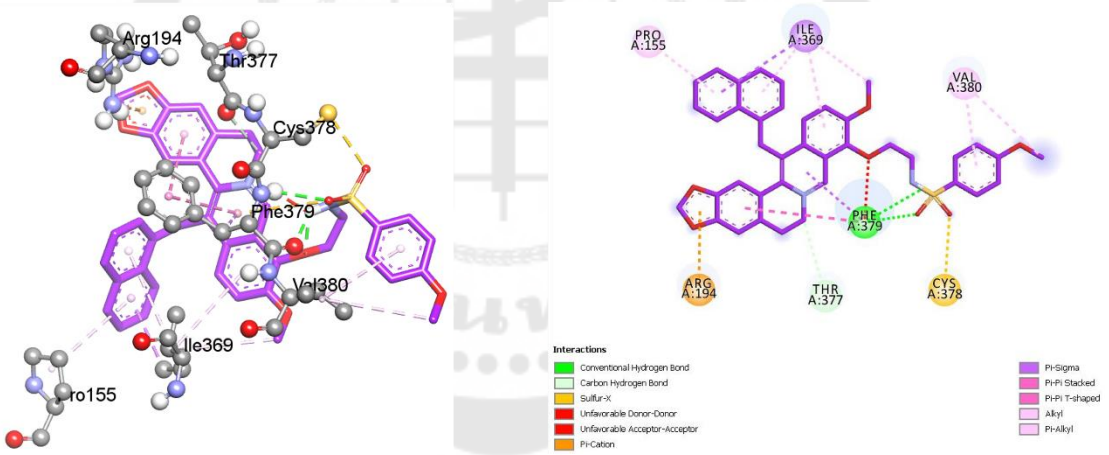

Figure 26 (A) Illustrates the 3D interactions of the best docking pose (compound **24**) on the surface of PCSK9 (B) 2D diagram of compound **24** interacted to PCSK9.

The binding mode of compound **12** was significantly different from BBR. The hydrophobic pockets were revealed in Figure 27 involving residues Ile369, Cys378, and Phe379. Furthermore, the C-6 position generated a hydrogen bond with Phe379. Interestingly, the key residue Thr377 generated a Pi-sulfur with ring D of BBR. Additionally, The OCH_3 of C-10 also interacted with residue Thr377 via hydrogen bond. Although compound **12** was bound to key amino acids, *in vitro* study showed that compound **12**

showed the lowest effect of PCSK9 expression. The results confirmed that the mode of binding played a vital role in PCSK9 inhibition efficiency.

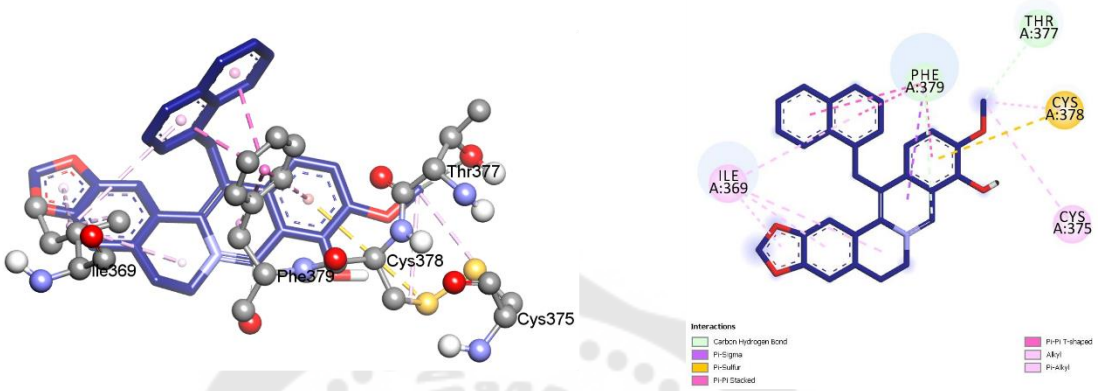

Figure 27 (A) Illustrates the 3D interactions of the best docking pose (compound **12**) on the surface of PCSK9 (B) 2D diagram of compound **12** interacted to PCSK9.

In contrast, the binding mode of compound **21** was also different from BBR. The naphthalene moiety occurred much hydrophobic interaction through Pro155, Ala239, Ile369, and Phe379. In addition, the ring D and ring C of the BBR core structure formed hydrophobic interaction via Ile369 and Phe379 residue, respectively. Besides, the sulfonamide group showed two hydrogen bonds with Phe379. Furthermore, the benzenesulfonyl moiety and *para*-methyl substituent generated hydrophobic interaction to the key residue Cys378, Phe379 as shown in Figure 28. Furthermore, compound **21** displayed similar PCSK9 inhibitory activity to compound **24**, as shown in Table 8. Interestingly, both compounds formed hydrophobic interactions with Pro155, Ile369 residues which might play an important role for enhance PCSK9 expression.

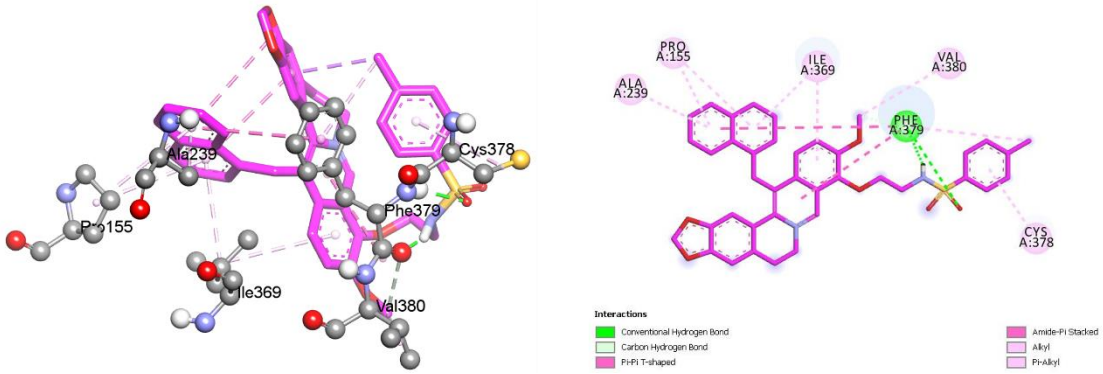

Figure 28 (A) Illustrates the 3D interactions of the best docking pose (compound **21**) on the surface of PCSK9 (B) 2D diagram of compound **21** interacted to PCSK9.

CHAPTER 5
SUMMARY AND SUGGESTION

A novel series of BBR derivatives as PCSK9 inhibitors were designed, synthesized, and evaluated their PCSK9 inhibition activity. To begin with, the introducing of aromaticity at the C-13 position and benzenesulfonyl moiety at the C-9 position could increase the lipophilicity of BBR. Then, the benzenesulfonyl ring was modified with different substituents on the *para*-position to improve the possibility of binding with key residues. The obtained results showed that all designed compounds exhibited strong binding interactions to PCSK9 than the parent BBR. Hence, the *in silico* study confirmed that most of the compounds fulfilled drug-likeness properties, except compound **24**. Finally, in order to determine the correlation between structure and activity relationships, the eight compounds were successfully synthesized. Furthermore, BBR derivatives that were substituted with the electron-donating group (compounds **21** and **24**) were generated in good yields. Unfortunately, substitution with electron-withdrawing group (compounds **27**, **30**, and **33**) occurred the unexpected product in the different ratio and could not separate to pure compounds. All synthesized compounds were confirmed their structures by NMR and MS spectroscopic data. BBR and its derivatives were treated with the HepG2 cells to investigate their cytotoxicity using MTT assay before evaluating PCSK9 inhibition assay. The results showed that BBR inhibited PCSK9 protein expression with 78% at 100 μmol/L, whereas the BBR derivatives that substituted with electron-donating group demonstrated more than 80% inhibition activity at 5 μmol/L. Thus, compounds **21** and **24** displayed a potent PCSK9 inhibitor. From molecular docking, both compounds were confirmed to interact with the key amino acids of PCSK9 with similar to BBR binding. Unfortunately, compound **24** was unfavorable to fit in the drug-likeness properties (MW and HBA counts). In conclusion, only the novel BBR derivatives **21** is suitable for further development as potential small molecule PCSK9 inhibitor for hypercholesterolemia treatment.

Suggestion

BBR derivatives substituted with an electron-withdrawing group will be synthesized using a protecting group for amine in future work. The synthetic plan is starting from using *tert*-Butyl carbamates (Boc) to protect the amine of bromoethylamine to form compound **45**. Next, compound **45** will react with compound **12** to give intermediate **46**, followed by adding a benzenesulfonyl chloride agent to generate **47**. In the final step, Boc will be removed under the acidic condition to get the desired compounds. The proposed mechanism is presented in Figure 29. All compounds will be purified and confirmed their structures by spectroscopic techniques.

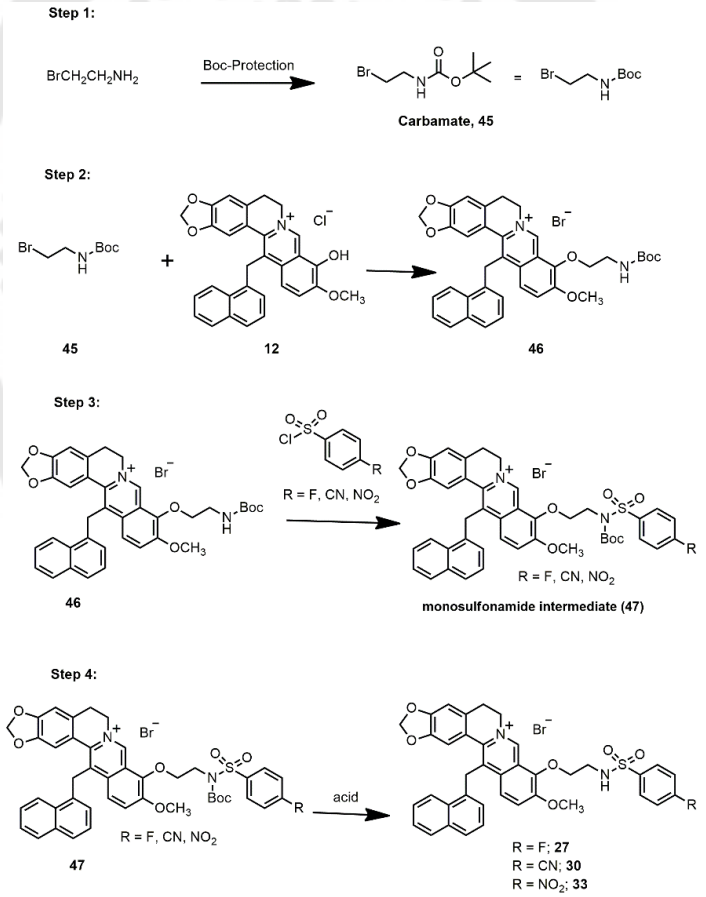

Figure 29 The proposed mechanism of an electron-withdrawing substituted BBR derivatives.

REFERENCES

Aggrey, M. O., Li, H. H., Wang, W. Q., Wang, Y., & Xuan, L. J. (2019). Indole alkaloid from Nauclea latifolia promotes LDL uptake in HepG2 cells by inhibiting PCSK9. *Phytomedicine, 55*, 264-268.

Alam, M. S., Nam, Y. J., & Lee, D. U. (2013). Synthesis and evaluation of (Z)-2,3-diphenylacrylonitrile analogs as anti-cancer and anti-microbial agents. *Eur J Med Chem, 69*, 790-797.

ALLEN R. LAST, J. D. F., ELIZABETH ROLLMANN MENZEL. (2017). Hyperlipidemia: Drugs for Cardiovascular Risk Reduction in Adults. *American Family Physician, 95*(2), 78-87.

American Heart Association, I. (2021). Heart disease and stroke statistics—2021 update: a report from the American

Heart Association. *Circulation*.

Bakht, M. A., Yar, M. S., Abdel-Hamid, S. G., Al Qasoumi, S. I., & Samad, A. (2010). Molecular properties prediction, synthesis and antimicrobial activity of some newer oxadiazole derivatives. *Eur J Med Chem, 45*(12), 5862-5869.

BIOVIA, D. S. (2020). discovery studio visualizer: San Diego: Dassault Systèmes,.

Cameron, J., Ranheim, T., Kulseth, M. A., Leren, T. P., & Berge, K. E. (2008). Berberine decreases PCSK9 expression in HepG2 cells. *Atherosclerosis, 201*(2), 266-273.

Dong, B., Li, H., Singh, A. B., Cao, A., & Liu, J. (2015). Inhibition of PCSK9 transcription by berberine involves down-regulation of hepatic HNF1alpha protein expression through the ubiquitin-proteasome degradation pathway. *J Biol Chem, 290*(7), 4047-4058.

Duff, C. J., & Hooper, N. M. (2011). PCSK9: an emerging target for treatment of hypercholesterolemia. *Expert Opin Ther Targets, 15*(2), 157-168.

Fala, L. (2016). Repatha (Evolocumab): Second PCSK9 Inhibitor Approved by the FDA for Patients with Familial Hypercholesterolemia. *American Health & Drug Benefits, 9*(Special Feature), 136.

G. M. Morris, R. H., W. Lindstrom, M. F. Sanner, R. K. Belew, D. S. Goodsell, A. J. Olson. (2009). AutoDock4 and AutoDockTools4: automated docking with selective receptor flexibility. *J. Comput. Chem, 30*, 2785–2791.

Gaba, S., Saini, A., Singh, G., & Monga, V. (2021). An insight into the medicinal attributes of berberine derivatives: A review. *Bioorg Med Chem, 38*, 116143.

He, N. Y., Li, Q., Wu, C. Y., Ren, Z., Gao, Y., Pan, L. H., . . . Liu, L. S. (2017). Lowering serum lipids via PCSK9-targeting drugs: current advances and future perspectives. *Acta Pharmacol Sin, 38*(3), 301-311.

Jaitrong, M. (2018). *DESIGN AND SYNTHESIS OF BERBERINE DERIVATIVES AS CHOLESTEROL LOWERING AGENT.* (Master degree). Srinakharinwirot university, Srinakharinwirot. (Chemistry).

Jeenduang, N. (2014). PCSK9: A New Target for Lipid-Lowering Therapy. *Songkla Med J, 32*(2), 89-105.

Jeon, H., & Blacklow, S. C. (2005). Structure and physiologic function of the low-density lipoprotein receptor. *Annu Rev Biochem, 74*, 535-562.

Jia, Y.-J., Xu, R.-X., Sun, J., Tang, Y., & Li, J.-J. (2014). Enhanced circulating PCSK9 concentration by berberine through SREBP-2 pathway in high fat diet-fed rats. *Journal of Translational Medicine, 12*(103).

Kong, W., Wei, J., Abidi, P., Lin, M., Inaba, S., Li, C., . . . Jiang, J. D. (2004). Berberine is a novel cholesterol-lowering drug working through a unique mechanism distinct from statins. *Nat Med, 10*(12), 1344-1351.

Kong, W. J., Wei, J., Zuo, Z. Y., Wang, Y. M., Song, D. Q., You, X. F., . . . Jiang, J. D. (2008). Combination of simvastatin with berberine improves the lipid-lowering efficacy. *Metabolism, 57*(8), 1029-1037.

Krahenbuhl, S., Pavik-Mezzour, I., & von Eckardstein, A. (2016). Unmet Needs in LDL-C Lowering: When Statins Won't Do! *Drugs, 76*(12), 1175-1190.

Lammi, C., Sgrignani, J., Roda, G., Arnoldi, A., & Grazioso, G. (2019). Inhibition of PCSK9(D374Y)/LDLR Protein-Protein Interaction by Computationally Designed T9 Lupin Peptide. *ACS Med Chem Lett, 10*(4), 425-430.

Li, D. D., Yu, P., Xu, H., Wang, Z. Z., Xiao, W., & Zhao, L. G. (2021). Discovery of C-9 Modified Berberine Derivatives as Novel Lipid-Lowering Agents. *Chem Pharm Bull (Tokyo), 69*(1), 59-66.

Li, H., Dong, B., Park, S. W., Lee, H. S., Chen, W., & Liu, J. (2009). Hepatocyte nuclear factor 1alpha plays a critical role in PCSK9 gene transcription and regulation by the natural hypocholesterolemic compound berberine. *J Biol Chem, 284*(42), 28885-28895.

M. J. Frisch, G. W. T., H. B. Schlegel, G. E. Scuseria, M. A. Robb, J. R. Cheeseman, G. Scalmani, V. Barone, B. Mennucci, G. A. Petersson, H. Nakatsuji, M. Caricato, X. Li, H. P. Hratchian, A. F. Izmaylov, J. Bloino, G. Zheng, J. L. Sonnenberg, M. Hada, M. Ehara, K. Toyota, R. Fukuda, J. Hasegawa, M. Ishida, T. Nakajima, Y. Honda, O. Kitao, H. Nakai, T. Vreven, J. A. Montgomery, J. E. Peralta, F. Ogliaro, M. Bearpark, J. J. Heyd, E. Brothers, K. N. Kudin, V. N. Staroverov, R. Kobayashi, J. Normand, K. Raghavachari, A. Rendell, J. C. Burant, S. S. Iyengar, J. Tomasi, M. Cossi, N. Rega, J.M. Millam, M. Klene, J. E. Knox, J. B. Cross, V. Bakken, C. Adamo, J. Jaramillo, R. Gomperts, R. E. Stratmann, O. Yazyev, A. J. Austin, R. Cammi, C. Pomelli, J. W. Ochterski, R. L. Martin, K. Morokuma, V. G. Zakrzewski, G. A. Voth, P. Salvador, J.J. Dannenberg, S. Dapprich, A. D. Daniels, Farkas, J. B. Foresman, J. V. Ortiz, J. Cioslowski, D. J. Fox. (2009). Gaussian 09, Revision B.01. *Gaussian, Inc.Wallingford CT*.

M.F. Sanner, P. (1999). a programming language for software integration and development. *J. Mol. Graphics Mod, 17*, 57-61.

Melendez, Q. M., Krishnaji, S. T., Wooten, C. J., & Lopez, D. (2017). Hypercholesterolemia: The role of PCSK9. *Arch Biochem Biophys, 625-626*, 39-53.

Nishikido, T., & Ray, K. K. (2018). Non-antibody Approaches to Proprotein Convertase Subtilisin Kexin 9 Inhibition: siRNA, Antisense Oligonucleotides, Adnectins, Vaccination, and New Attempts at Small-Molecule Inhibitors Based on New Discoveries. *Front Cardiovasc Med, 5*, 199.

Ogura, M. (2018). PCSK9 inhibition in the management of familial hypercholesterolemia. *J Cardiol, 71*(1), 1-7.

Patel, P. (2021). A bird's eye view on a therapeutically 'wonder molecule': Berberine. *Phytomedicine Plus, 1*(3), 100070.

Petersen, D. N., Hawkins, J., Ruangsiriluk, W., Stevens, K. A., Maguire, B. A., O'Connell, T. N., . . . Carpino, P. A. (2016). A Small-Molecule Anti-secretagogue of PCSK9 Targets the 80S Ribosome to Inhibit PCSK9 Protein Translation. *Cell Chem Biol, 23*(11), 1362-1371.

Pirillo, A., & Catapano, A. L. (2015). Berberine, a plant alkaloid with lipid- and glucose-lowering properties: From in vitro evidence to clinical studies. *Atherosclerosis, 243*(2), 449-461.

Puratchikody, A., Irfan, N., & Balasubramaniyan, S. (2019). Conceptual design of hybrid PCSK9 lead inhibitors against coronary artery disease. *Biocatalysis and Agricultural Biotechnology, 17*, 427-440.

Seidah, N. G., Awan, Z., Chretien, M., & Mbikay, M. (2014). PCSK9: a key modulator of cardiovascular health. *Circ Res, 114*(6), 1022-1036.

Song, K. H., Kim, Y. H., Im, A. R., & Kim, Y. H. (2018). Black Raspberry Extract Enhances LDL Uptake in HepG2 Cells by Suppressing PCSK9 Expression to Upregulate LDLR Expression. *J Med Food, 21*(6), 560-567.

Soran, H., Dent, R., & Durrington, P. (2017). Evidence-based goals in LDL-C reduction. *Clin Res Cardiol, 106*(4), 237-248.

Sultan Alvi, S., Ansari, I. A., Khan, I., Iqbal, J., & Khan, M. S. (2017). Potential role of lycopene in targeting proprotein convertase subtilisin/kexin type-9 to combat hypercholesterolemia. *Free Radic Biol Med, 108*, 394-403.

Taechalertpaisarn, J., Zhao, B., Liang, X., & Burgess, K. (2018). Small Molecule Inhibitors of the PCSK9.LDLR Interaction. *J Am Chem Soc, 140*(9), 3242-3249.

Virani, S. S., Alonso, A., Benjamin, E. J., Bittencourt, M. S., Callaway, C. W., Carson, A. P., . . . Stroke Statistics, S. (2020). Heart Disease and Stroke Statistics-2020 Update: A Report From the American Heart Association. *Circulation, 141*(9), e139-e596.

Wu, C., Xi, C., Tong, J., Zhao, J., Jiang, H., Wang, J., . . . Liu, H. (2019). Design, synthesis, and biological evaluation of novel tetrahydroprotoberberine derivatives (THPBs) as proprotein convertase subtilisin/kexin type 9 (PCSK9) modulators for the treatment of hyperlipidemia. *Acta Pharm Sin B, 9*(6), 1216-1230.

Xie, H., Yang, K., Winston-McPherson, G. N., Stapleton, D. S., Keller, M. P., Attie, A. D., . . . Tang, W. (2020). From methylene bridged diindole to carbonyl linked benzimidazoleindole: Development of potent and metabolically stable PCSK9 modulators. *Eur J Med Chem, 206*, 112678.

Xu, S., Luo, S., Zhu, Z., & Xu, J. (2019). Small molecules as inhibitors of PCSK9: Current status and future challenges. *Eur J Med Chem, 162*, 212-233.

Appendix

A) Calculating $IC_{50}$of cytotoxicity of selected compounds (A) BBR, (B) Compound **2**, (C) Compound **12**, (D) Compound **14**, (E) Compound **21**, and (F) Compound **24** in HepG2 cells.

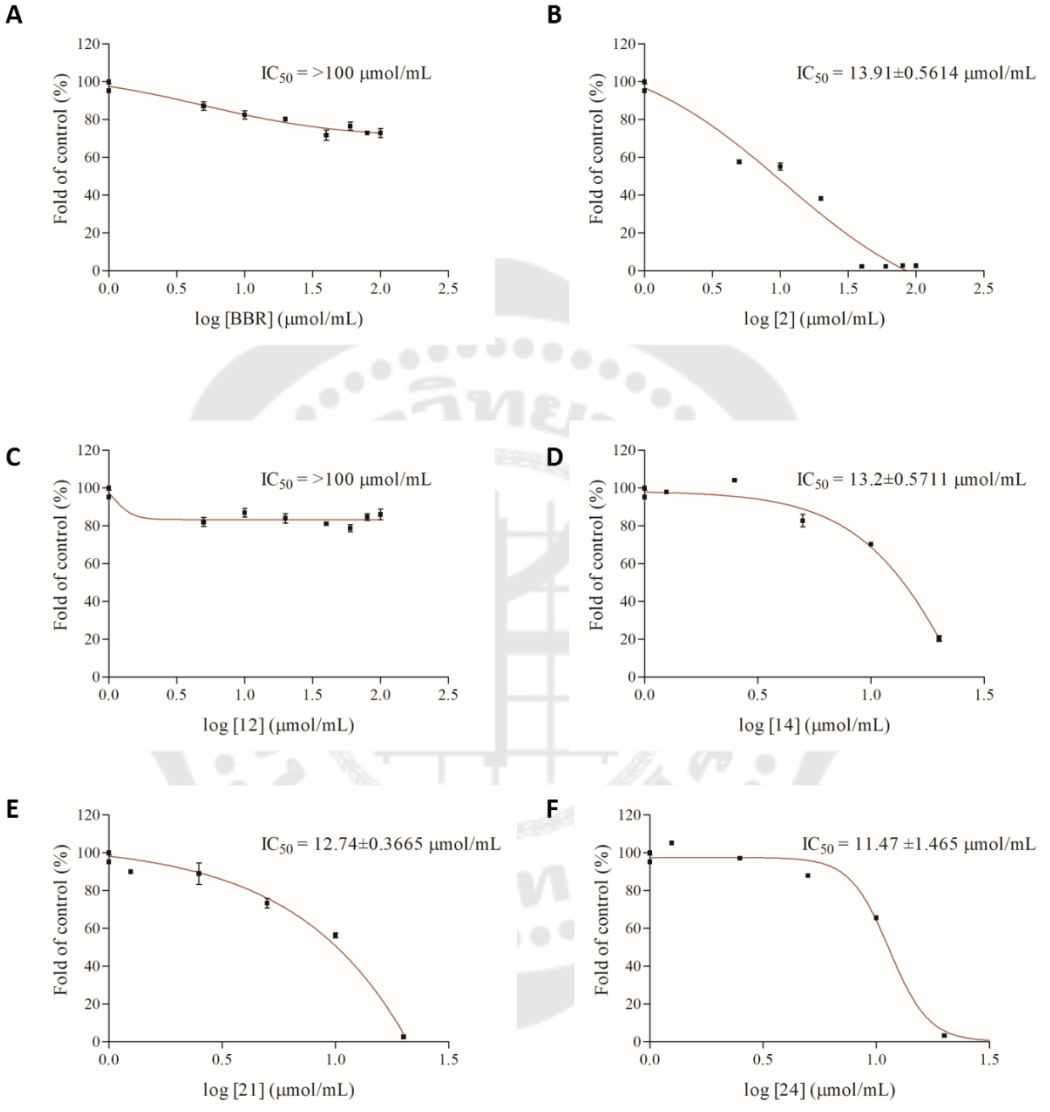

B) Copies of ^{1}H NMR spectra of all target compounds.

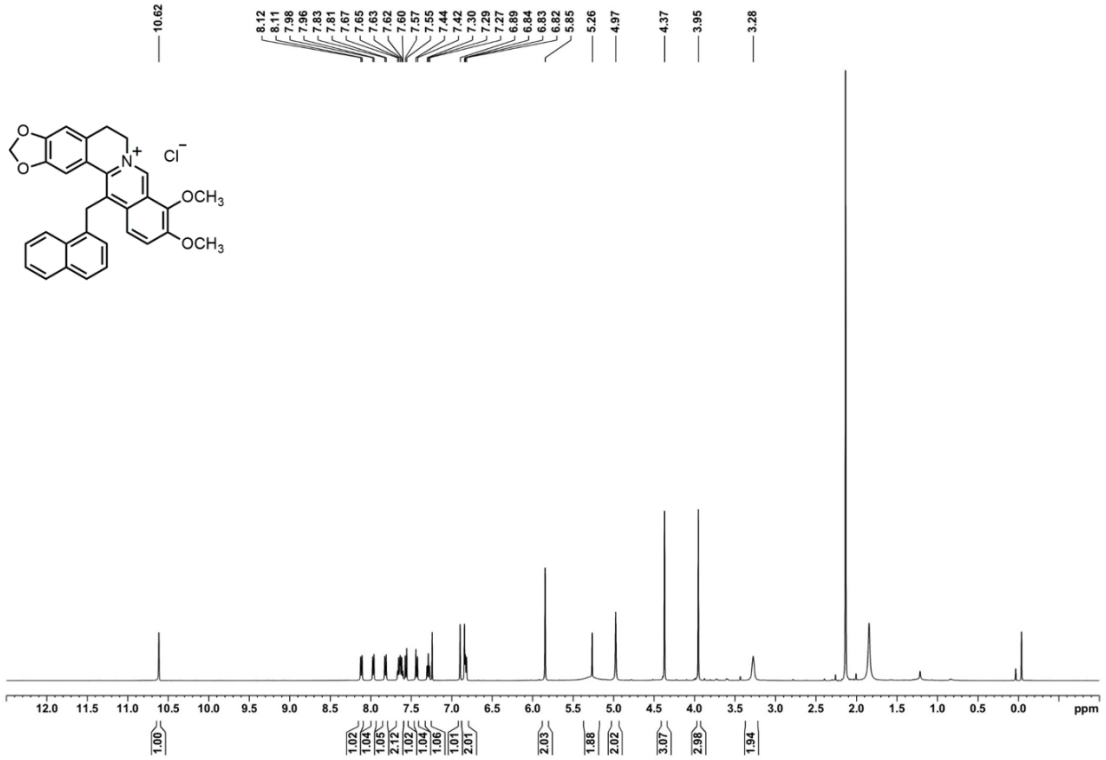

Figure 30 ^{1}H –NMR of compound **2** in $CDCl_3$

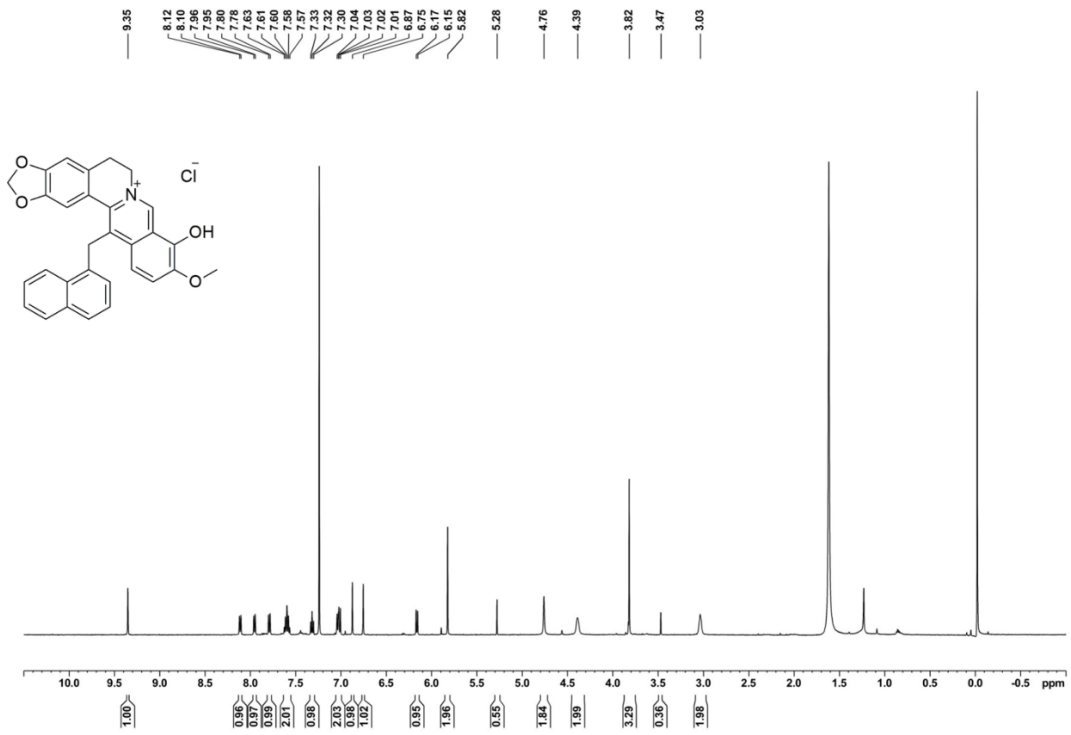

Figure 31 ^{1}H –NMR of compound **12** in $CDCl_3$

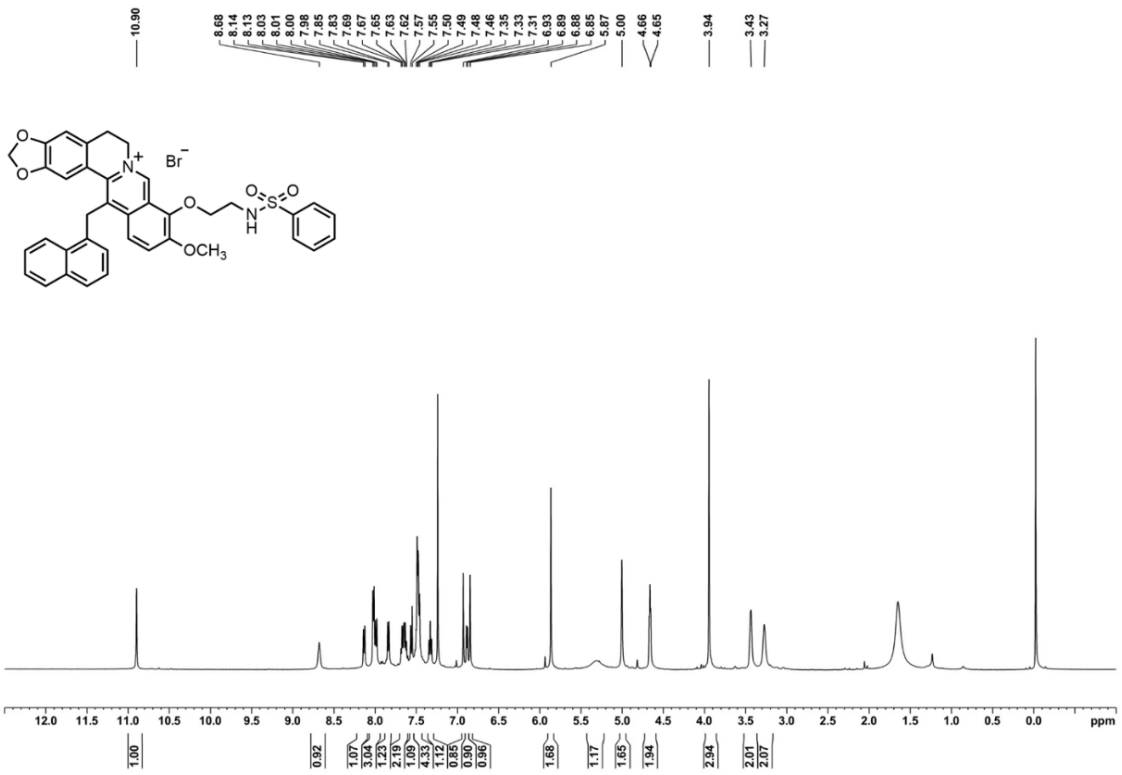

Figure 32 ^{1}H –NMR of compound **14** in $CDCl_3$

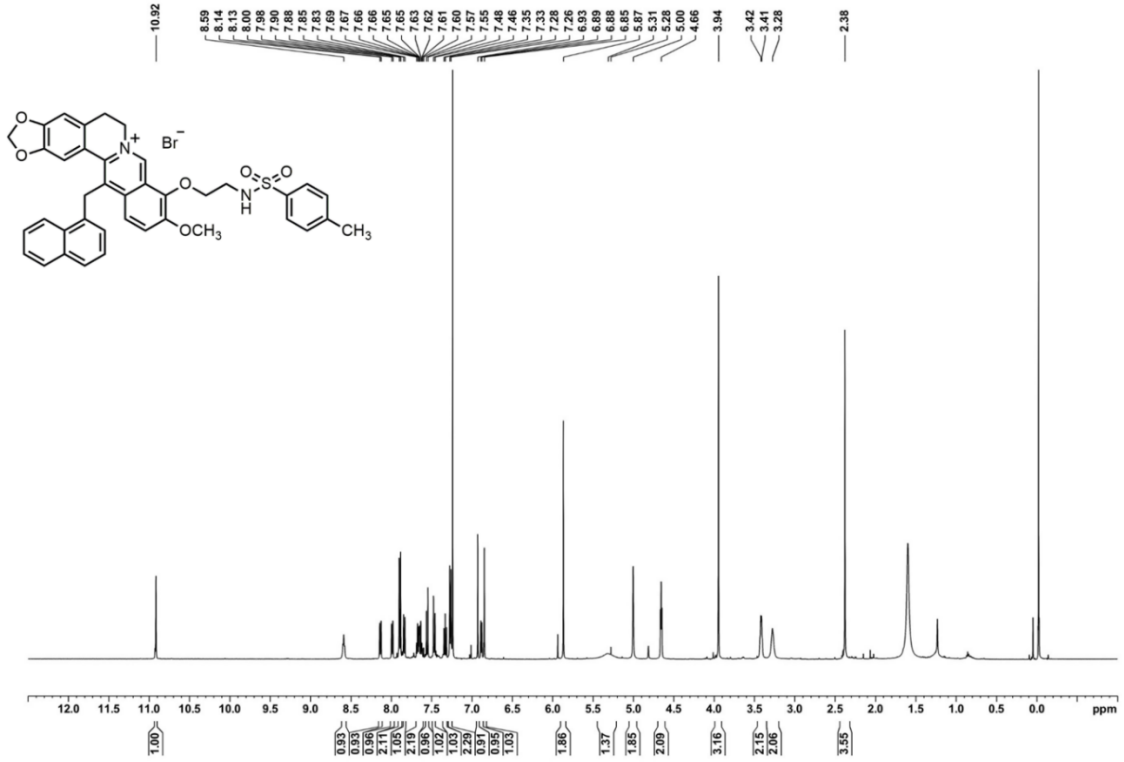

Figure 33 ^{1}H –NMR of compound **21** in $CDCl_3$

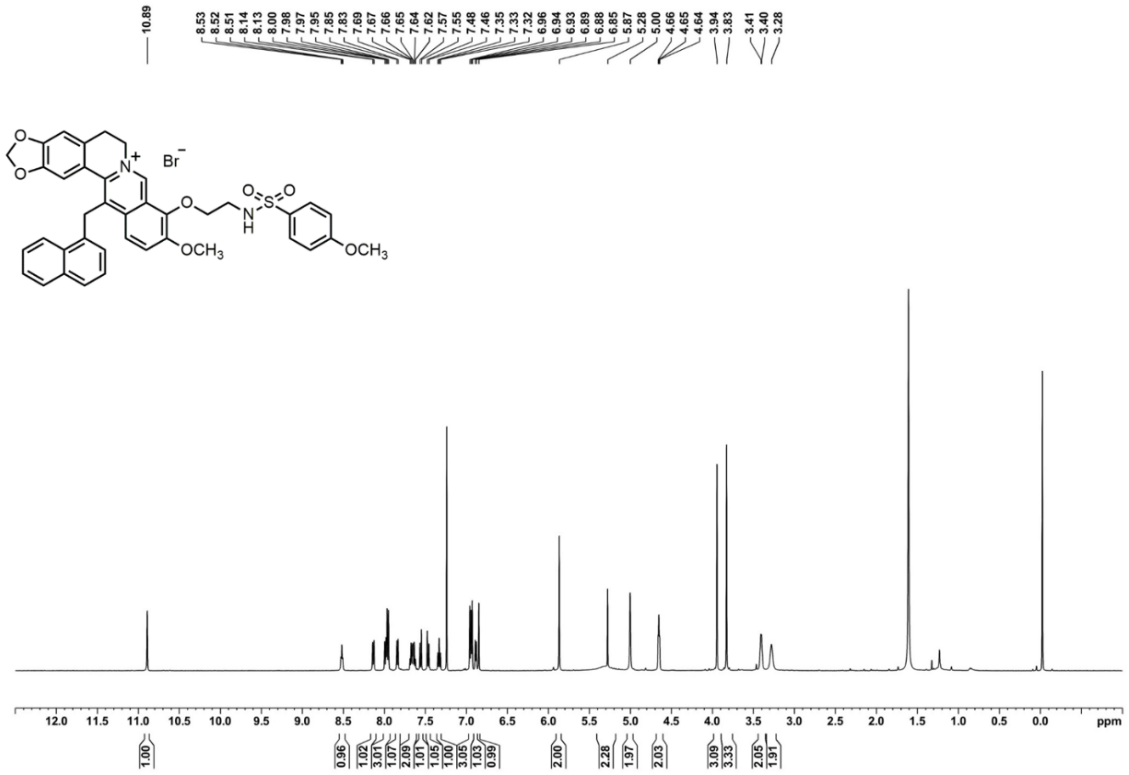

Figure 34 ^{1}H –NMR of compound **24** in $CDCl_3$

C) Copies of ESI-HR-MS spectra of all target compounds.

Mass Spectrum SmartFormula Report

Analysis Info

Analysis Name	D:\Data\Siritorn\ESI\SS-HRMS 6 (pos).d	Acquisition Date	7/4/2021 12:19:39 PM
Method	tune_low_ pos.m	Operator	RU
Sample Name	st2214	Instrument	micrOTOF 8213750.10411
Comment			

Acquisition Parameter

Source Type	ESI	Ion Polarity	Positive	Set Nebulizer	2.0 Bar
Focus	Not active			Set Dry Heater	200 °C
Scan Begin	50 m/z	Set Capillary	4500 V	Set Dry Gas	8.0 l/min
Scan End	2000 m/z	Set End Plate Offset	-500 V	Set Divert Valve	Waste

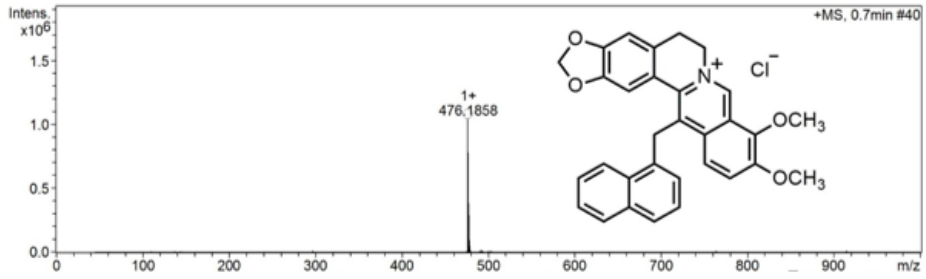

Formula Calculator Results

m/z	Calc m/z	Diff (mDa)	Diff (ppm)	Ion Formula
476.1858	476.1856	0.2	0.4	C31H26NO4

Mass Spectrum SmartFormula Report

Analysis Info

Analysis Name	D:\Data\Siritorn\ESI\SS-HRMS 5 (pos).d	Acquisition Date	7/4/2021 12:13:12 PM
Method	tune_low_ pos.m	Operator	RU
Sample Name	st2207	Instrument	micrOTOF 8213750.10411
Comment			

Acquisition Parameter

Source Type	ESI	Ion Polarity	Positive	Set Nebulizer	2.0 Bar
Focus	Not active			Set Dry Heater	200 °C
Scan Begin	50 m/z	Set Capillary	4500 V	Set Dry Gas	8.0 l/min
Scan End	2000 m/z	Set End Plate Offset	-500 V	Set Divert Valve	Waste

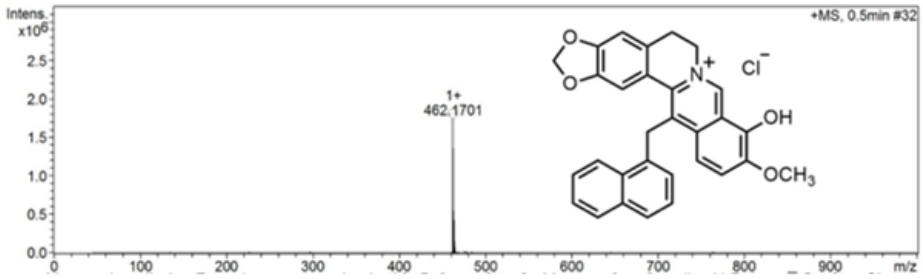

Formula Calculator Results

m/z	Calc m/z	Diff (mDa)	Diff (ppm)	Ion Formula
462.1701	462.1700	0.1	0.3	C30H24NO4

Mass Spectrum SmartFormula Report

Analysis Info

Analysis Name	D:\Data\Siritorn\ESI\SS-HRMS 4 (pos).d	Acquisition Date	7/4/2021 12:03:39 PM
Method	tune_low_ pos.m	Operator	RU
Sample Name	MJ220	Instrument	micrOTOF 8213750.10411
Comment			

Acquisition Parameter

Source Type	ESI	Ion Polarity	Positive	Set Nebulizer	2.0 Bar
Focus	Not active			Set Dry Heater	200 °C
Scan Begin	50 m/z	Set Capillary	4500 V	Set Dry Gas	8.0 l/min
Scan End	2000 m/z	Set End Plate Offset	-500 V	Set Divert Valve	Waste

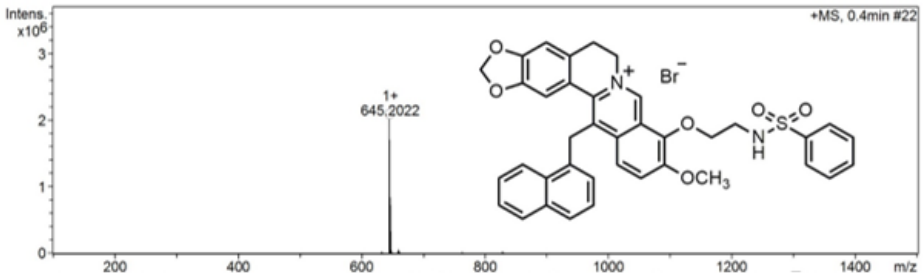

Formula Calculator Results

m/z	Calc m/z	Diff (mDa)	Diff (ppm)	Ion Formula
645.2022	645.2054	3.2	-5.0	C38H33N2O6S

Mass Spectrum SmartFormula Report

Analysis Info

Analysis Name	D:\Data\Siritorn\ESI\SS-HRMS 3 (pos).d	Acquisition Date	7/4/2021 11:56:47 AM
Method	tune_low_ pos.m	Operator	RU
Sample Name	MJ214	Instrument	micrOTOF 8213750.10411
Comment			

Acquisition Parameter

Source Type	ESI	Ion Polarity	Positive	Set Nebulizer	2.0 Bar
Focus	Not active			Set Dry Heater	200 °C
Scan Begin	50 m/z	Set Capillary	4500 V	Set Dry Gas	8.0 l/min
Scan End	2000 m/z	Set End Plate Offset	-500 V	Set Divert Valve	Waste

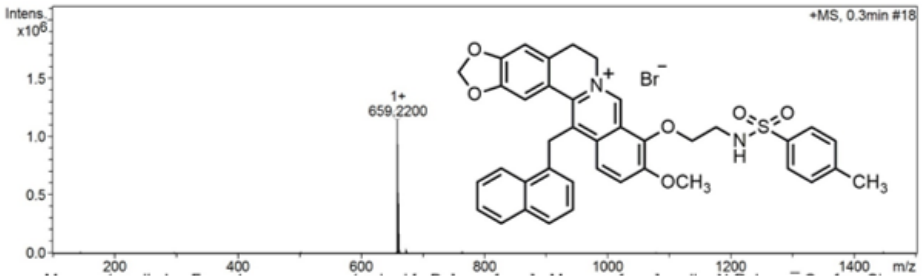

Formula Calculator Results

m/z	Calc m/z	Diff (mDa)	Diff (ppm)	Ion Formula
659.2200	659.2210	1.0	1.5	C39H35N2O6S

Mass Spectrum SmartFormula Report

Analysis Info

Analysis Name	D:\Data\Siritorn\ESI\SS-HRMS 10 (pos).d	Acquisition Date	7/4/2021 12:45:47 PM
Method	tune_low_ pos.m	Operator	RU
Sample Name	MJ245	Instrument	micrOTOF 8213750.10411
Comment			

Acquisition Parameter

Source Type	ESI	Ion Polarity	Positive	Set Nebulizer	2.0 Bar
Focus	Not active			Set Dry Heater	200 °C
Scan Begin	50 m/z	Set Capillary	4500 V	Set Dry Gas	8.0 l/min
Scan End	2000 m/z	Set End Plate Offset	-500 V	Set Divert Valve	Waste

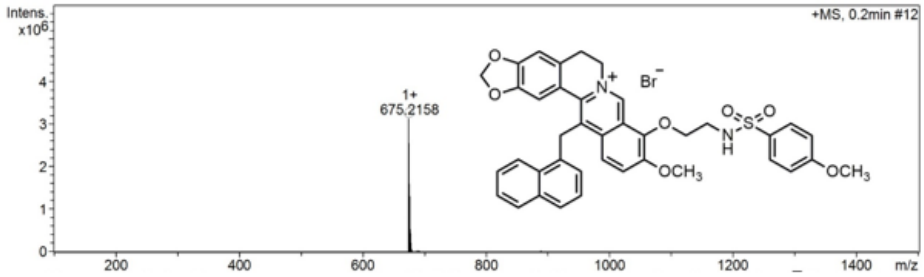

Formula Calculator Results

m/z	Calc m/z	Diff (mDa)	Diff (ppm)	Ion Formula
675.2158	675.2159	0.2	- 0.2	C39H35N2O7S

VITA

NAME	Munchalika Jaitrong
DATE OF BIRTH	10 August 1995
PLACE OF BIRTH	Chonburi
INSTITUTIONS ATTENDED	Srinakharinwirot University
HOME ADDRESS	21/845 Sattahip, Sattahip, Chonburi 20180
PUBLICATION	Molecular Docking Studies of Berberine Derivatives as Novel Multitarget PCSK9 and HMGCR Inhibitors